CONTRIBUTIONS FROM THE MUSEUM OF PALEONTOLOGY

THE UNIVERSITY OF MICHIGAN

Vol. 25, No. 3, p. 45-87 (7 text-figs.; 6 plates) January 26, 1979

THE ONTOGENY AND TAXONOMY OF THE MISSISSIPPIAN BLASTOID GENUS *SCHIZOBLASTUS*

BY

DONALD B. MACURDA, JR.
MUSEUM OF PALEONTOLOGY
THE UNIVERSITY OF MICHIGAN

MUSEUM OF PALEONTOLOGY
THE UNIVERSITY OF MICHIGAN
ANN ARBOR

CONTRIBUTIONS FROM THE MUSEUM OF PALEONTOLOGY

Gerald R. Smith, Director

Robert V. Kesling, Editor

Diane Wurzinger, Editor for this number

The series of contributions from the Museum of Paleontology is a medium for the publication of papers based chiefly upon the collection in the Museum. When the number of pages issued is sufficient to make a volume, a title page and a table of contents will be sent to libraries on the mailing list, and to individuals upon request. A list of the separate papers may also be obtained. Correspondence should be directed to the Museum of Paleontology, The University of Michigan, Ann Arbor, Michigan, 48109.

VOLS. II–XXV. Parts of volumes may be obtained if available. Price lists available upon inquiry.

THE ONTOGENY AND TAXONOMY OF THE MISSISSIPPIAN BLASTOID GENUS *SCHIZOBLASTUS*

By

Donald B. Macurda, Jr.[1]

Abstract.– The Mississippian blastoid genus *Schizoblastus*, characterized by extensive development of the deltoid to form part of the thecal wall, has four species: *S. aplatus* (Rowley and Hare, 1891); *S. marginulus* (Rowley, 1901); *S. moorei* (Cline, 1936); and *S. sayi* (Shumard, 1855). The genus is known only from Osagean strata. The four species are principally found in Missouri, although *S. sayi* ranges from Kentucky to New Mexico. Measurements reveal that growth relations between thecal plates are linear. Restudy of older collections clarifies synonyms of some species and refines our knowledge of the distribution of *Schizoblastus*.

INTRODUCTION

The blastoid *Schizoblastus* Etheridge and Carpenter, 1882, is a widely distributed genus in the lower Mississippian of the United States, ranging from Kentucky to New Mexico. Because its vertical distribution throughout these areas is limited, it is useful biostratigraphically. *Schizoblastus* is unusual amongst the blastoids in the moderate to extremely large development of the deltoids which are usually confined to the upper portion of the theca in most blastoid genera.

The type species of *Schizoblastus, S. sayi*, was first described from Missouri by Shumard in 1855. Subsequent workers extended the distribution of *S. sayi* throughout Missouri and into Iowa, Illinois, Oklahoma, and Arkansas. In addition, it has been found in New Mexico and Kentucky, thereby considerably extending its range. Numerous synonyms were also proposed for *S. sayi*. Between 1891 and 1901 two additional different species of *Schizoblastus* were described from northeastern Missouri: *S. aplatus* (Rowley and Hare) and *S. marginulus* (Rowley). These species are apparently confined to this area. In 1936 Cline reviewed the systematics and biogeography of *Schizoblastus* and offered several new combinations of names and species including *S. moorei* Cline from southwestern Missouri. The range of this species has subsequently been extended into northwestern Arkansas and probably western Illinois.

This paper is a continuation of a series on the morphology, distribution, and taxonomy of Mississippian blastoids. Globose blastoids with long ambulacra are the most common forms in lower Mississippian rocks, representing an extensive evolutionary experiment by blastoids. When the morphology and distribution of these forms and their precursors is adequately known, it will be possible to state these evolutionary sequences in some detail.

[1] Present address: Exxon Production Research Corporation, Houston, Texas, 77001

THE GROWTH SERIES

Five growth series of *S. sayi* from the Burlington Limestone and Reeds Spring Formation were analyzed during this study. The populations span a linear distance of 300 miles, from Burlington, Iowa to Reeds Spring, Missouri, in a northeast-southwest direction. Stratigraphic control on these collections vary. The series (A) from Burlington, Iowa (n = 22), was collected in the nineteenth century by a number of collectors and must be considered as coming from anywhere within the Burlington Limestone in a radius of fifteen miles of Burlington (see Appendix 1). Those (series B) from Hannibal, Missouri (n = 15) which is 100 miles south of Burlington, were collected by the writer over a three-year period from a restricted ten-foot interval (lower *Physetocrinus* Zone) in the Burlington Limestone at one locality (lateral extent approximately 2,000 feet). Those (series E) from Louisiana, Missouri (n = 15) were collected around the turn of the century from the upper Burlington Limestone at Louisiana, Missouri, 20 miles southeast of Hannibal, by R. R. Rowley. Since the occurrence of *Schizoblastus sayi* is approximately the same at these localities, his collections are probably from a limited stratigraphic interval but range geographically around Louisiana. The series (D) from central Missouri (n = 11) is a composite from two Burlington Limestone quarries fifteen miles apart west of Columbia and north of Sedalia, Missouri, about 100 miles southwest of Hannibal. These were collected by L. M. Cline and L. R. Laudon. The fifth series (C; n = 18) was collected by Cline, Laudon, Beane, and Renfro from the upper Reeds Spring Formation at its type locality in southwest Missouri, 140 miles south of the central Missouri localities. The only criterion for placing specimens in the sample to be measured was that the desired characters be measurable (growth series B-D) or in the case of larger original populations that the length alone be somewhat different from that of a specimen previously admitted (series A and E). This procedure follows that utilized in other blastoid growth studies (*e.g.*, Breimer and Macurda, 1972) and provides an unbiased estimate of the total range of development and variation. The number of unadmitted specimens varies, from 5 for locality D (out of 16) to approximately 11 of 29 for locality C, and approximately 40 of 55 for locality B, reflecting the vagaries of preservation, weathering, and ease of collection. The statistics derived from these samples thus analyze assemblages that range from undoubtedly contemporaneous populations (series B and probably C) to those varying in time and space (series A and D). Plotted regression lines are quite similar for the five populations of *S. sayi* (text-figs. 3B; 4A, C; 5B). Only single populations are available for the other species. Illustrations and explanations for the symbols are given in Macurda (1967) and Breimer and Macurda (1972).

In addition to the illustrations of the growth series for *Schizoblastus*, that of a former species, *S. melonoides* (Meek and Worthen, 1869) now assigned to *Decemoblastus* (Macurda, 1977), are given for comparative purposes (text-figs. 6A-F; 7A-E).

STRATIGRAPHIC DISTRIBUTION

Schizoblastus was defined on the basis of the species *S. sayi* (Shumard, 1855) by Etheridge and Carpenter (1882). The other species which they referred to the genus were Mississippian or lower Carboniferous in age (1886). Cline reviewed the generic concept of *Schizoblastus* in 1936 and noted that all the species which he could refer to the genus were either from the Mississippian of North America or the Permian of Timor. The latter species have since been grouped under *Deltoblastus* by Fay (1961a). Bassler and Moodey (1943) assigned numerous other Mississippian species to *Schizoblastus* but only two of these belong to the genus as presently understood. The subsequent disposition of the other species is as follows:

1) *S. burlingtonensis* Cline, 1936 = *S. sayi*. SUI 776. (Herein).
2) *S. cornutus* (Meek and Worthen, 1861) = *Cribroblastus cornutus*. Fay, 1961b.

3) *S. curtus* (Shumard, 1855) = *nomina dubia.* Macurda, 1978.
4) *S. decussatus* (Shumard, 1858) = *Xenoblastus decussatus.* Breimer and Macurda, 1972.
5) *S. etheridgei* Cline, 1936 = *Decemoblastus melonoides* (Meek and Worthen, 1869). Macurda, 1977.
6) *S. incisus* Hambach, 1903 = *Cryptoblastus melo* (Owen and Shumard, 1850). USNM S3721. (Herein).
7) *S. laudoni* Cline, 1936 = *S. sayi.* SUI 778. (Herein).
8) *S. lotoblastus* (White, 1877). USNM 8541. The specimen is not well preserved. The anal area is apparently an anispiracle; the number of hydrospires is unknown. The species is currently unidentifiable generically.
9) *S. melonoides* (Meek and Worthen, 1869) = *Decemoblastus melonoides.* Macurda, 1977.
10) *S. neglectus* (Meek and Worthen, 1869) = *Lophoblastus neglectus.* Macurda, 1967.
11) *S. schucherti* (Hambach, 1903). USNM 35410. Poorly preserved crackout fauna. Generic identification indeterminate.
12) *S. tenuistriatus* (Hambach, 1903) = *Lophoblastus neglectus*? Macurda, 1962.

Macurda (1962) assigned two additional species to *Schizoblastus, S. aplatus* and *S. marginulus,* bringing the total now assigned to four.

Schizoblastus aplatus is known only from the Burlington Limestone (Osagean). It has only been found in the upper Burlington along the Mississippi River in northeastern Missouri and adjacent counties in western Illinois (Macurda, 1962); it occurs in the *Cactocrinus* and lower *Physetocrinus* zones of Laudon (1937; see also Rowley, 1908). *Schizoblastus marginulus* is also restricted to the same region (Macurda, 1962), occurring in the *Cactocrinus* zone (Rowley, 1908). *Schizoblastus moorei* was originally described from the Reeds Spring Formation in southwestern Missouri. It also occurs in northwestern Arkansas and in approximately correlative Osagean units in western Illinois (Pl. 2, fig. 8). *Schizoblastus sayi* has the widest geographic distribution of the four species. It is common in the upper Burlington Limestone from southeastern Iowa to southwestern Missouri; it also occurs in the Reeds Spring Formation of southwestern Missouri, the Boone Group in northern Arkansas, the St. Joe Limestone of northeastern Oklahoma, the Nunn (Pl. 3, fig. 13), Tierra Blanca, and Dona Ana members of the Lake Valley Formation in the Sacramento Mountains of New Mexico, and the Borden Formation in Kentucky (Pl. 3, fig. 12), and about three and one-half miles east of Berea, Kentucky on Kentucky Highway 21. The label for the last named occurrence was given as the Conway Siltstone Member of the Broadhead Formation; this interval is approximately equal to that now mapped as the Cowbell Member of the Borden Formation (Weir, 1967). These occurrences are all Osagean in age.

SPECIES DIFFERENTIATION

Schizoblastus sayi is readily recognized by its long deltoid and can be differentiated from specimens of *S. moorei* with long deltoids by the presence of a trough between the ridges bordering the spiracles, running continuously from the deltoid lip to the deltoid body (Pl. 5, fig. 5) whereas this same area is elevated in *S. moorei* (Pl. 1, fig. 2). Macurda (1962, pp. 1375-1376) gave the following characteristics which distinguish between *S. aplatus, S. marginulus,* and *S. moorei.* In *S. moorei* a broad thick ridge borders the ambulacra; there is no ridge on the deltoid of *S. aplatus* and the bordering ridge in *S. marginulus* is quite sharp and keel-like. *S. moorei* has a longer deltoid than that of *S. aplatus* and much coarser deltoid ornamentation than that of *S. marginulus*; it is also larger

than either of those species. These characters will readily differentiate *S. moorei* from the above species.

S. aplatus can be differentiated from *S. marginulus* by the following:

1) base – prominent stem attachment in nine of ten specimens of *S. marginulus*; none in *S. aplatus*;
2) deltoids – no rim bordering ambulacra in *S. aplatus*; sharp, keel-like in *S. marginulus*;
3) deltoid ornamentation – nodose (spikes if preservation is excellent) in *S. aplatus*; fine growth lines in *S. marginulus*;
4) spiracles – inclined toward one another in *S. aplatus*, not separated from rest of deltoid by a ridge; axis parallel to that of adjacent ambulacrum in *S. marginulus* and separated from the rest of the deltoid by a sharp ridge.

PALEOECOLOGY

Schizoblastus is a globose blastoid; the length and convexity of the ambulacra would have allowed the brachioles to be extended through an arc of nearly 270-300°. No brachioles or columns have been preserved intact. Based upon the relatively few known columns and brachioles preserved in blastoids, an estimate of a column 10 cm long and brachioles 3 cm long might be reasonable for a large *S. sayi* (thecal length approximately 20 mm).

It is inferred that *Schizoblastus* had a root system at the base of its column because of the kinds of substrates on which it occurs. The Burlington Limestone is a crinoidal grainstone; however, the horizons in which *S. sayi* reaches its greatest abundance in northeastern Missouri are often very fine-grained skeletal debris. *S. aplatus* and *S. marginulus* are also restricted to the Burlington Limestone. I have not been able to develop any precise bathymetric depths for the Burlington Limestone, but my estimates, based upon sedimentary structures and bedform and firsthand experience with modern crinoids and their environments, are that water depths in the Burlington ranged from a few meters to a few tens of meters. The lower part of the *Physetocrinus* zone in which *S. sayi* reaches its greatest abundance is probably a somewhat quieter or deeper water environment than usual in the Burlington. *S. sayi* also occurs in the clastics of the Broadhead and New Providence Formations in Kentucky but is very rare, being known from only two specimens. In New Mexico it occurs in the Nunn, Tierra Blanca, and Dona Ana members of the Lake Valley Formation. These are high-energy deposits of crinoidal grainstones that accumulated around the bioherms which are developed in the Sacramento Mountains. Echinoderms apparently grew as halos around the bioherms and were carried to deeper water upon death. Specimens of *S. sayi* are very rare from here. *S. moorei* occurs in the Reeds Spring Formation of southwestern Missouri along with *S. sayi*. These species can be found together in the same bed. The substrates are carbonate but little detailed information is available concerning local environments.

SYSTEMATIC PALEONTOLOGY

Class BLASTOIDEA

Order SPIRACULATIDA Jaekel, 1921

Family *Schizoblastidae* Etheridge and Carpenter, 1886

Genus *Schizoblastus* Etheridge and Carpenter, 1882

Schizoblastus Etheridge and Carpenter, 1882, p. 243, 1886, p. 220; Bather, 1900, p. 92; Wanner, 1924, p. 40; Cline, 1936, p. 263; Bergounioux, 1953, p. 647; Fay, 1961b, p. 100; Fay and Wanner, 1967, p. S427.

Type species.— *Pentremites sayi* Shumard, 1855 (by subsequent designation, Etheridge and Carpenter, 1886).

Generic diagnosis.— Spiraculate blastoids with ten spiracles, those in CD interarea separate from anal opening; two anal deltoids, an epi- and hypodeltoid. Theca globose-ellipsoidal; ambulacra extend almost to base of theca; basals flat-slightly convex. Narrow external exposure of lancets along most of ambulacral length. Ten hydrospire groups, two hydrospires per group. One pore between adjacent side plates along radial and, occasionally, present and functional along deltoid margin. Deltoids well developed, forming one-third to two-thirds of thecal length, usually overlap radials. *Mississippian*, Arkansas, Illinois, Iowa, Kentucky, Missouri, and New Mexico.

Remarks.— *Schizoblastus* belongs to the family Schizoblastidae, to which Fay and Wanner (1967) assigned seven genera. *Acentrotremites* (L. Carb.) has been reassigned to the fissiculate blastoids (Breimer and Macurda, 1972) and *Strongyloblastus* has been shown to be a Mississippian genus belonging to the family Pentremitidae (Macurda and Breimer, 1977). The remaining five genera are Mississippian (*Auloblastus, Lophoblastus, Orbiblastus, Schizoblastus*) or Permian (*Deltoblastus*) in age. *Auloblastus* has four anal deltoids, four hydrospires per group, ambulacra which extend the full length of the theca, and concave basalia; *Lophoblastus* has two anal deltoids, three hydrospires per group, ambulacra which extend three-quarters of the thecal length, and convex basalia; *Orbiblastus* has two anal deltoids, three hydrospires per group, ambulacra which extend the full length of the theca, and concave basalia; *Deltoblastus* has two anal deltoids, two hydrospires per group, ambulacra which extend the full length of the theca, and concave basalia. As Fay (1961a) noted, the only genus closely allied in form to *Schizoblastus* is *Deltoblastus*. The latter differs in having the radials overlap the deltoids, the ambulacra are petaloid in broad ambulacral sinuses, with nearly the full width of the lancet exposed, the basal concavity is deeply concave, and the deltoid septa extend into oral crests (Fay, 1961a).

Schizoblastus aplatus (Rowley and Hare)

Pl. 1, figs. 8, 10, 11, 14; Pl. 3, figs. 3-6, 8-11;

Pl. 5, fig. 9; Pl. 6, fig. 3

Granatocrinus aplatus Rowley and Hare, 1891, p. 117, Pl. 3, figs. 11, 12.
Orbitremites aplatus Bather, 1899, p. 24.
Lophoblastus aplatus Rowley, 1901, p. 346.
Schizoblastus aplatus Macurda, 1962, p. 1373, text-fig. 4A-C.

Description.— Thecae small, globose in lateral view with slight flattening near base; and hood of hypodeltoid projects orally (Pl. 3, figs. 4, 6). Ambulacra convex, long, reaching almost to base of theca. Pelvis short, broad, flat to very slightly convex (Pl. 3, figs. 5, 9). Theca rounded pentagonal to rounded decagonal in oral view (Pl. 3, figs. 3, 8), greatest width equatorial. Length and width of theca nearly equal (text-fig. 1A; Table 1).

Basalia three, small, in normal position, forming one-half of pelvis, confined to base of theca (Pl. 3, fig. 10). Lateral outline of basalia flat to very slightly convex with slight indentation at center for stem cicatrix; outline in plan view decagonal. Stem cicatrix a simple, very slightly depressed circle at inner part of basalia, 0.5–0.7 mm in diameter. Center of basalia pierced by a narrow lumen.

Azygous basal rhombic in plan view, with straight lateral sides and very slightly convex distal edges. Each BR sector very slightly convex parallel to and flat to very slightly concave perpendicular to BR axis. Adjacent sectors meet over flat to slightly convex surface in center of basal; laterally each sector merges with its neighboring lateral sector of the zygous basal over a flat to very slightly concave surface. Zygous basals pentagonal in plan view with straight lateral and distal lateral edges and a very slightly concave distal medial edge. Medial BR sector is slightly convex parallel to and

TABLE 1 – Growth relationships of principal variables of *Schizoblastus aplatus* (Rowley and Hare), n = 14. See Macurda, 1966, 1967 for explanation and illustration of symbols for variables.

Variables	r	a_0	a_1	Observed range (mm) y	Observed range (mm) x
L/W	0.90	0.40	0.86	3.5 – 7.6	3.0 – 7.5
L/Amb. L.	0.99	0.22	1.06	3.5 – 7.6	3.0 – 6.9
ABBR/RB	0.65	0.52	0.38	0.7 – 1.2	0.6 – 1.5
ABBR/RD	0.90	0.44	0.15	0.7 – 1.2	1.8 – 5.1
ABBR/Del. L.	0.89	0.42	0.17	0.7 – 1.2	1.7 – 4.5
RD/RDF	0.90	0.73	2.37	1.8 – 5.1	0.5 – 1.6
RR/RRF	0.70	0.37	0.20	0.6 – 1.4	2.0 – 5.2
RB/RBF	0.86	0.00	1.35	0.6 – 1.5	0.5 – 1.0
RD/RR	0.71	0.53	2.51	1.8 – 5.1	0.6 – 1.4
RD/RB	0.83	0.27	2.96	1.8 – 5.1	0.6 – 1.5
RR/RB	0.81	0.23	0.82	0.6 – 1.4	0.6 – 1.5
RD/Del. L.	0.95	0.00	1.10	1.8 – 5.1	1.7 – 4.5
RB/Del. L.	0.87	0.15	0.28	0.6 – 1.5	1.7 – 4.5
RD/Σ	0.98	-0.27	0.67	1.8 – 5.1	3.2 – 7.8
RR/Σ	0.83	-0.20	0.16	0.6 – 1.4	3.2 – 7.8
RB/Σ	0.91	0.07	0.17	0.6 – 1.5	3.2 – 7.8
Del. L./Del. Gr. Ab. W.	0.95	0.72	1.20	1.7 – 4.5	0.8 – 3.0
Amb. L./ No. S. P.	0.97	-0.82	0.27	3.0 – 6.9	13 – 28

r = correlation coefficient (y, x), a_0 = y intercept, a_1 = regression coefficient.

strongly convex perpendicular to medial BR axis (strongly convex ridge begins distal to the stem cicatrix). Lateral BR sectors very slightly convex parallel to and flat to very slightly concave perpendicular to lateral BR axis. Strong medial ridge of central sector of zygous basals continues into radials (Pl. 3, fig. 5); other BR sectors merge smoothly with adjacent RB sectors. Rates of growth of BR and RB axes slow, equal; that of RD axis and deltoid much faster than BR (text-fig. 1B, E). ABBRF: 0.7–1.3 mm. See also Table 1.

Radials five, body short, limbs elongate. Outline of radial pentagonal in plan view, with slightly convex lower edge, slightly convex lateral edges which expand in width adorally, and two very slightly concave distal edges which slant inward toward ambulacrum; parabolic radial sinus penetrates nearly to base of plate. Radial quadrate in lateral view with convex edge bordering ambulacrum, slightly convex edge facing proximally, slightly concave lower edge, and a very slightly concave adoral facing edge. Origin of radial obscured by a lip of calcite at aboral end of ambulacrum; rim in inner part of RD sector borders ambulacrum; crest of rim ornamented with pointed nodes (Pl. 3, figs. 4, 6); height of top of nodes equals that of ambulacrum. RB sector small, very slightly convex parallel

and perpendicular to RB axis. RB sectors merge over convex ridge on C and E radials, slightly more subdued on other radials; each RB sector merges with adjacent RR sector over a very slightly convex surface. RR sector very slightly convex parallel to and strongly convex perpendicular to RR axis; RR sector merges smoothly with RD sector. Latter convex parallel to and very slightly convex perpendicular to RD axis. Growth lines only faintly expressed in RB sector, slightly more distinct in RR sector; those in RD sector occasionally bear rows of pointed nodes. Occasional pointed nodes scattered through RR and RB sectors. RD grows at a faster rate than RR and RB which are nearly equal; there is no apparent shift in growth rates with increasing age (text-fig. 1C, D, F, G). Length of RB axis equal to width of its growth front while RD axis is longer than the width of its growth front; the RR axis is shorter than its growth front (text-fig. 1I). Rate of growth of RD equal to that of deltoid (text-fig. 1B). See also Table 1 for measurements of radials.

Deltoids four, together with epideltoid forming border of peristome. Deltoid outline triangular in plan view, extending one-third of length of theca, convex in lateral view, and very slightly convex to very slightly concave in cross section (Pl. 1, figs. 8,10). Adoral edge of deltoid bordering peristome straight, width expanding aborally along straight DDF, then contracting along suture with lancet, reaching minimum exposed width at spiracles; width of deltoid body expands along straight suture with ambulacra; aboral borders (DRF) with radials very slightly convex. Deltoid lip bears strong V-shaped, adorally pointing rim which forms border to ambulacral tract and projects into oral area (Pl. 1, fig. 10); adoral face of rim bears minor grooves of ambulacral tract. Immediately behind rim deltoid drops into two troughs which lead into two spiracles which are slightly recessed. Deltoid body rhombic in outline, with adoral pointed end beginning just behind rim of deltoid lip and narrowly separating the two spiracles; width of deltoid body expands aborally to its maximum width at the radiodeltoid suture. Deltoid body is ornamented by coarse, short, sharp nodes (Pl. 1, figs. 8, 14; Pl. 3, fig. 11). Occasionally the nodes are more subdued, occurring atop growth lines which parallel the aboral margins of the plate. The nodes may also occur as three or four rows which are radially aligned. Aboral rate of growth of deltoid faster than the expansion of its width (text-fig. 1J). Del. L.: 1.7–4.5 mm; Gr. Ad. W.: 0.5–1.2 mm; Min. W.: 0.1–0.5 mm; Gr. Ab. W.: 0.8–3.0 mm.

Anal deltoids two, an epi- and hypodeltoid. Outline of epideltoid as for deltoid lip of regular deltoid except for embayment of aboral edge of plate by anal opening. Upper surface of epideltoid formed into a massive horseshoe-shaped rim which forms adoral border to anal opening (Pl. 1, figs. 10, 11). Adoral face of epideltoid rim bears minor grooves of ambulacral tract. Outline and ornament of hypodeltoid as for deltoid body except for adoral end which is embayed by anal opening and formed into a hood which projects above anal opening 0.4–1.2 mm (Pl. 1, figs. 11, 14; Pl. 3, fig. 11). Anal opening circular to ovoid, bordered adorally by epideltoid, aborally by hypodeltoid, with axis of opening directed upward and adorally. Anus L.: 0.5–0.8 mm; Anus W.: 0.5–0.7 mm. Area of anal opening does not increase much with increasing size of the viscera (text-fig. 5C).

Ambulacra five, linear, moderately long, reaching nearly to base of theca, gradually tapering in width aborally (Pl. 5, fig. 9). Strongly convex in lateral view; convex in cross section except for concavity along ambulacral tract. Ambulacra slightly elevated above level of surrounding plates except for nodes on rim of RD sector of radials and nodes of deltoid. Lancet does not quite reach peristome, shape conforms to that of ambulacrum but it is narrower; lancet is exposed over one-third of ambulacral width at adoral end of ambulacrum; width of exposure decreases aborally; not exposed aboralmost 1.0–1.5 mm of ambulacral length. Side plates triangular in plan view, with slightly convex edge bordering lancet; adoral edge straight, extending from lancet abmedially to radial or deltoid; bordered on inner one-third of suture by adjacent side plate, on outer two-thirds by outer side plate. Aboral edge of side plate is bordered by next aboral side plate, adoral edge of an outer side plate, and a hydrospire pore; each edge straight; plate edge bends adorally going from lancet to edge of ambulacrum. Relatively large triangular outer side plate present, bordered laterally by radial or deltoid, adorally by hydrospire pore and a side plate, and aborally by another side plate.

Hydrospire pore small, ovoid-triangular, bordered laterally by radial (pores absent along deltoid), adorally by side plate, aborally by outer side plate. Arcuate pore furrow leads into hydrospire pore. Absence of pores along deltoid due to continued lateral growth of side plates and outer side plates. Small ovoid brachiolar facet, sited on outer sloping edge of ambulacrum on side plate and outer side plate. Three – four minor grooves border main groove per side plate; two – three minor grooves border adoral margin of side groove as well (Pl. 6, fig. 3). Traces of oral cover plates preserved in one specimen (Pl. 1, fig. 11). Ambulacral length increases during ontogeny; approximately 4 side plates per mm (text-fig. 1H). Amb. L.: 3.0–6.9 mm; Amb. W.: 0.9–1.5 mm; No. S. P.: 13–28. Number of brachioles increases as volume of viscera increases (text-fig. 3D).

Ten spiracles, those in anal interarea well separated from anal opening. Regular spiracles teardrop-shaped, slightly recessed, adoral edge 0.5–1.1 mm from center of peristome; length 0.2–0.3 mm; width 0.1–0.2 mm. Spiracle bordered adorally and on one side by deltoid, on other side by lancet and side plates. Adoral ends of spiracles can be closely set. Anal spiracles set back farther from center of peristome, bordered adorally by epideltoid, laterally by hypodeltoid on one side and by lancet and side plates on other side. Two hydrospires per ambulacral side.

Peristome pentagonal.

Remarks.– The above description is based upon the fourteen specimens in the growth series (Appendix 1).

Hydrospires were determined from RX-36D, where they were seen in a broken D ambulacrum and a detached polished radial with the A ambulacrum (Macurda, 1962).

One specimen (not in the growth series) has irregularities in the development of the A and B ambulacra, the interambulacral space being very narrow, and the ambulacra shortened and crooked.

See SPECIES DIFFERENTIATION for a comparison between this and other species assigned to *Schizoblastus*.

Schizoblastus marginulus (Rowley)

Pl. 2, figs. 12-21; Pl. 6, fig. 1

Lophoblastus marginulus Rowley, 1901, p. 345, Pl. 38, figs. 18, 19.
Schizoblastus marginulus Macurda, 1962, p. 1374, text-fig. 5A, B, C.

Description.– Theca globose in lateral view with slight flattening at summit and flattened at base (Pl. 2, fig. 16). Ambulacra convex, long, almost reaching to base of theca. Pelvis short, broad;

(Opposite Page)

TEXT-FIG. 1 – Growth series of *Schizoblastus aplatus* (Rowley and Hare) and *Schizoblastus marginulus* (Rowley). Slope of lines fitted by regression equation in form of Y = A + BX. See tables for values of equations. *S. aplatus*: *A*, Length of theca vs. width; *B*, Lengths of RD and BR growth axes vs. deltoid length; *C*, Lengths of RD and RR growth axes vs. total growth of radial axes; *D*, Length of RB growth axis vs. total growth of radial axes; *E*, Length of BR growth axis vs. lengths of RD and RB growth axes; *F*, Triangular diagram showing percent of total radial growth of RD, RR, and RB growth axes; note poles have different values; *G*, Lengths of RD and RB growth axes vs. length of RR growth axis; *H*, Ambulacral length vs. number of side plates per ambulacral side; *I*, Lengths of RD, RR, and RB growth axes vs. widths of their respective growth fronts; *J*, Deltoid length vs. greatest aboral deltoid width. *S. marginulus*: *K*, Lengths of RD and RB growth axes vs. length of RR growth axis; *L*, Ambulacral length vs. number of side plates per ambulacral side; *M*, Length of theca vs. width; *N*, Deltoid length vs. greatest aboral deltoid width; *O*, Length of BR growth axis vs. lengths of RD and RB growth axes.

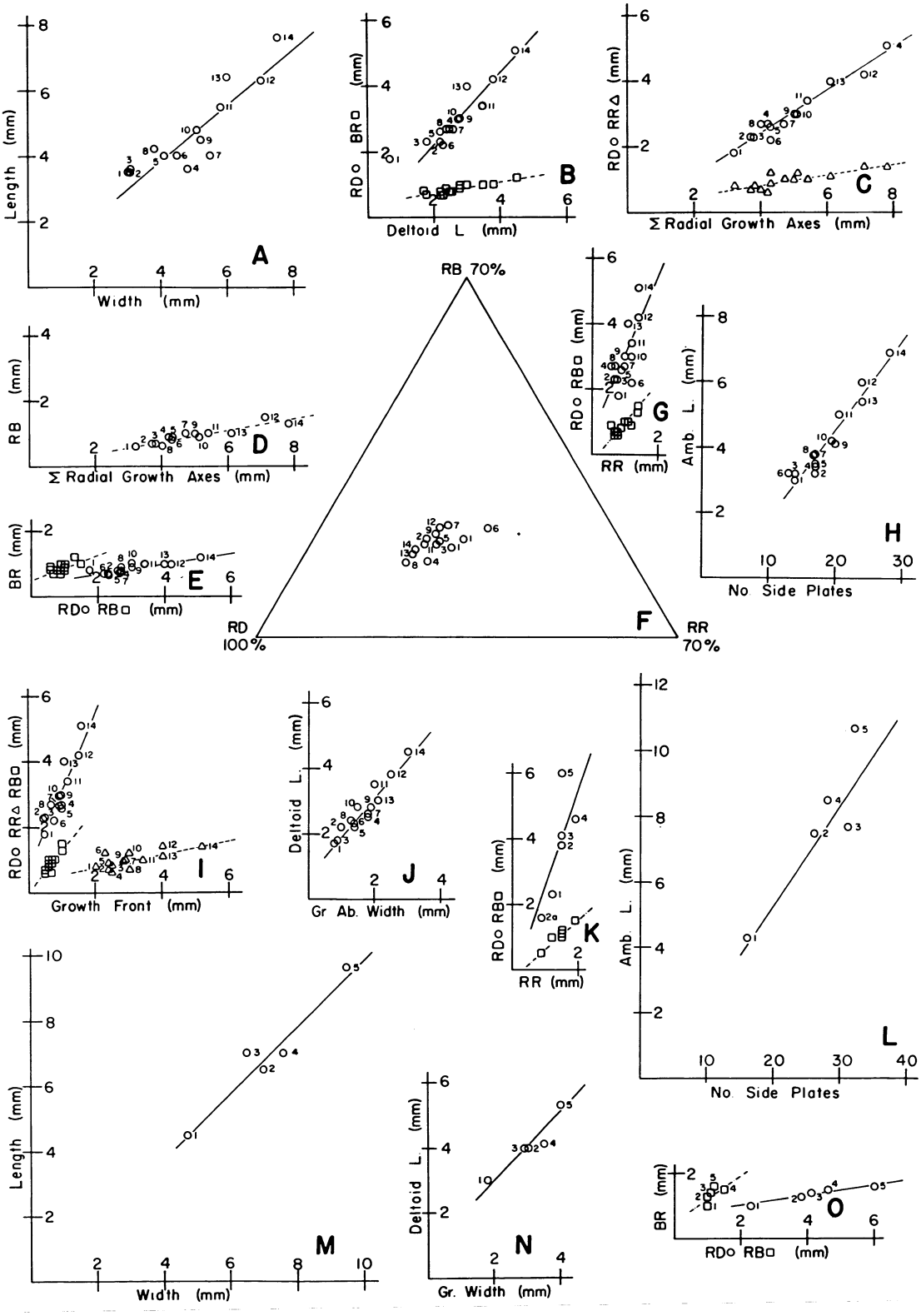
A
Length (mm)
Width (mm)
B
RDo BRo (mm)
Deltoid L (mm)
C
RDo RRΔ (mm)
Σ Radial Growth Axes (mm)
D
RB (mm)
Σ Radial Growth Axes (mm)
E
BR (mm)
RDo RBo (mm)
F
RB 70%
RD 100%
RR 70%
G
RDo RBo (mm)
RR (mm)
H
Amb. L. (mm)
No Side Plates
I
RDo RRΔ RBo (mm)
Growth Front (mm)
J
Deltoid L. (mm)
Gr Ab. Width (mm)
K
RDo RBo (mm)
RR (mm)
L
Amb. L. (mm)
No. Side Plates
M
Length (mm)
Width (mm)
N
Deltoid L (mm)
Gr. Width (mm)
O
BR (mm)
RDo RBo (mm)

column attachment area slightly protuberant (Pl. 2, figs. 12, 16, 17, 21). Theca rounded pentagonal to pentagonal in oral view with slightly concave interambulacral areas and protuberant narrow ambulacra (Pl. 2, figs. 13, 15); greatest width equatorial. Thecae small, length and width almost equal (text-fig. 1M, Table 2).

Basalia small, forming one-half of pelvis whose diameter ranges from 4.2–6.2 mm. Basalia confined to base of theca. Lateral outline of basalia slightly convex, recurved near outer edge; outline in plan view octagonal. Inner half of basals covered by a well-developed triangular-ovoid secondary deposit of calcite (diameter: 1.5–2.0 mm) which is elevated above the surrounding level of the basals (Pl. 2, fig. 21); edge can be slightly frilly. Crenellar ring in center of deposit very slightly concave, diameter 1.0 mm. Center of basalia pierced by a small round lumen.

Azygous basal rhombic in plan view, with straight lateral edges and very slightly convex distal edges (Pl. 2, fig. 21). Distal to secondary calcite, each BR sector slightly convex parallel to and slightly convex to convex perpendicular to BR axis. Adjacent BR sectors meet over a flat to concave surface and also merge with adjacent lateral BR sectors of ZB through a slightly concave to concave arc. Zygous basals pentagonal in plan view with straight lateral edges, slightly convex distal lateral edges, and a very slightly concave distal medial edge (Pl. 2, fig. 21). Distal to secondary calcite, medial BR sector very slightly convex or sinusoidal parallel to BR axis and convex perpendicular to it. Lateral BR sectors straight parallel and perpendicular to BR axis, merge with medial BR sector on flat to very slightly convex surface. Portions of basals distal to secondary deposit ornamented by strong growth lines which parallel radial-basal sutures. Rate of growth of BR axis nearly equal to that of RB axis but much slower than RD axis and deltoid (text-figs. 1O, 2C; Table 2). ABL: 1.3–2.0 mm; ABW: 1.1–1.8 mm; ABBBF: 0.7–1.2 mm; ABBRF: 1.1–1.5 mm.

Radials five, body very short, limbs of moderate length, extending slightly above equator of theca (Pl. 2, fig. 18). Outline of radial in plan view is quadrate, with slightly convex lower edge, lateral edges convex in lower part, becoming straighter adorally, upper edges very slightly concave, sloping slightly upward in an adoral direction from lateral edges. Radial sinus of moderate length, reaching nearly to base of plate, sides nearly parallel. In lateral view outline of radial is quadrate, with long convex edge bordering ambulacrum, short slightly concave edge in BR sector, concave edge along interradial suture, and slightly concave edge facing deltoid. There is a lip of secondary calcite which obscures the origin of the radial at aboral tip of ambulacrum and there is a strong rim to the ambulacrum which rises upward from the inner edge of the RD sector (Pl. 2, fig. 18). Rim smooth, not rising as high as midline of ambulacrum. RB sector small, varying from very slightly convex to very slightly concave parallel to and flat perpendicular to RB axis; adjacent RB sectors merge over convex surface. RR sectors straight parallel to and convex (more so in lower part) perpendicular to RR axis; merge with adjacent RB sector over flat to very slightly concave surface and with adjacent RD sector over flat to very slightly convex surface. RD sector convex parallel to and slightly concave perpendicular to RD axis. All sectors ornamented by strong growth lines parallel to radial sutures. Rate of growth of RR axis slightly greater than RB axis; RD has highest rate of growth and accelerates with age (text-figs. 1K, 2E, G). Width of RBF equal to RB while RR much shorter than RRF and RD much longer than RDF (text-fig. 2D). Rate of growth of RD nearly equal to deltoid (text-fig. 2C). For measurements of radial, see Table 2.

Deltoids four, together with epideltoid forming border to peristome; relatively large, extending nearly to equator of theca. Deltoid quadrate in plan view, convex in lateral view, concave laterally and flat medially in cross section (Pl. 2, fig. 20). Deltoid lip small, with straight adoral edge bordering peristome; DDR straight, diverging along centerline of ambulacral tract; deltoid lip contracts along concave suture with ambulacrum (first lancet, then side plates) to adoral end of spiracles; deltoid body then expands adorally along straight edge bordering ambulacrum to maximum width at radiodeltoid suture; radiodeltoid sutures very slightly convex. Adoral part of deltoid lip has elevated triangular area with two short ridges which extend aborally to adoral end of spiracle; trough between

TABLE 2 – Growth relationships of principal variables of *Schizoblastus marginulus* (Rowley), n = 5. See Macurda, 1966, 1967 for explanation and illustration of symbols for variables.

Variables	r	a_0	a_1	Observed range (mm) y	Observed range (mm) x
L/W	0.97	-0.22	1.01	4.5 – 9.6	4.7 – 9.5
L/Amb. L.	0.98	0.94	0.77	4.5 – 9.6	4.3 – 10.7
ABBR/RB	0.64	0.54	0.71	1.0 – 1.6	1.0 – 1.5
ABBR/RD	0.96	0.67	0.17	1.0 – 1.6	2.3 – 6.0
ABBR/Del. L.	0.92	0.30	0.25	1.0 – 1.6	3.1 – 5.5
RD/RDF	0.98	-0.28	2.41	2.3 – 6.0	1.0 – 2.5
RR/RRF	0.49	1.10	0.11	1.2 – 1.9	2.2 – 5.4
RB/RBF	0.77	0.30	0.86	1.0 – 1.5	0.8 – 1.2
RD/RR	0.55	-0.34	2.96	2.3 – 6.0	1.2 – 1.9
RD/RB	0.52	0.23	3.38	2.3 – 6.0	1.0 – 1.5
RR/RB	0.89	0.28	1.07	1.2 – 1.9	1.0 – 1.5
RD/Del. L.	0.98	-2.44	1.55	2.3 – 6.0	3.1 – 5.5
RB/Del. L.	0.37	0.77	0.09	1.0 – 1.5	3.1 – 5.5
RD/Σ	0.97	-1.32	0.80	2.3 – 6.0	4.5 – 8.7
RR/Σ	0.72	0.77	0.11	1.2 – 1.9	4.5 – 8.7
RB/Σ	0.37	0.77	0.09	1.0 - 1.5	3.1 – 5.5
Del. L./Del. Gr. Ab. W.	0.95	1.09	1.04	3.1 – 5.5	1.9 – 4.0
Amb. L./No. S. P.	0.91	-0.98	0.33	4.3 – 10.7	16 – 32

r = correlation coefficient (y, x), a_0 = y intercept, a_1 = regression coefficient.

ridges extends aborally between spiracles to deltoid body. Rim, a continuation of that on radial, borders each edge of deltoid body, becomes narrow, sharp and high adjacent to spiracle. Deltoid body wedge-shaped, being concave in cross section in adoral part, becoming flat medially in aboral part; surface turns up strongly into rim bordering ambulacrum. Deltoid body ornamented by strong growth lines which parallel radiodeltoid suture and turn adorally to form part of rim, indicating addition of calcite on lateral edges of deltoid body with growth as in *S. sayi*. Deltoid grows faster in an aboral direction than its width expands (text-fig. 1N). Del. L.: 3.1–5.5 mm, Gr. Ad. W.: 0.9–1.1 mm; Min. W.: 0.4–0.7 mm; Gr. Ab. W.: 1.9–4.0 mm.

Anal deltoids two, an epi- and hypodeltoid (Pl. 2, figs. 14, 19). Configuration of epideltoid as for deltoid lip except for medial indentation of aboral edge by anal opening; upper surface of epideltoid forms a massive rim to anal opening, adoral tip of which projects over peristome. Epi-hypodeltoid suture occurs midway on septa forming border between anal opening and adjacent spiracles. Configuration of hypodeltoid as for deltoid body except for adoral end where indentation by anal opening; surface of plate rises upward aboral to anal opening, forming a hood. Adoral end

of hypodeltoid thus the highest point of the theca, forming an elevated pyramidal area which drops vertically into anus and slopes downward aborally to merge into hypodeltoid body. Anal opening ovoid, bordered adorally by epideltoid, aborally by hypodeltoid, directed upward and inward toward point above oral area. Anus L.: 0.7–0.9 mm; Anus W.: 0.5–0.6 mm. Data too limited to show any clear relationship between volume of viscera and area of anal opening (text-fig. 4F).

Ambulacra five, long, linear, narrow, extending from near peristome almost to base of theca; strongly convex in lateral view; 3-4 side plates per mm (text-fig. 1L). Ambulacrum convex in cross section with concavity along median part of ambulacral tract (Pl. 6, fig. 1). Ambulacrum elevated above rim surrounding radials but becoming even with rim of bordering deltoids except for pronounced rim of spiracle which is elevated above it. Lancet extending almost to peristome, exposed along median one-fourth to one-fifth of ambulacrum almost to aboral tip of ambulacrum. Each side plate quadrate, wide medially, pointed laterally, with slightly convex medial edge bordering lancet, a straight adoral edge, and two straight aboral edges, inner one bordering next side plate, with outer edge bordering quadrate outer side plate. Tapered outer edge of side plate borders radial or deltoid as does relatively wide outer edge of outer side plate. Edges of outer side plate border two adjacent side plates, radial or deltoid, and ambulacral pore. Triangular ambulacral pore bordered by radial laterally, outer side plate aborally, and side plate orally. Pores functional along both radials and deltoids. Short arcuate pore furrow leads into each hydrospire pore. Brachiolar facets small, ovoid, 0.3 by 0.2 mm, sited on side and outer side plates along outer sloping edge of ambulacrum. 3-4 minor grooves per side plate border main ambulacral groove (Pl. 6, fig. 1) and 3-4 border side groove between main groove and brachiolar facet; the 3-4 on the adoral side of each side groove are more strongly developed than those on the aboral side.

Ten spiracles, those in anal interarea being well separated from the anal opening externally. Regular spiracles teardrop-shaped, narrow, elongate, bordered adorally and laterally on one side by deltoid, on other side laterally by side plates of ambulacrum; adoral edge 1.0–1.5 mm from center of peristome. Shape of two anal spiracles identical, bordered adorally by epideltoid, laterally on one side by epi- and hypodeltoid, and laterally on other side by side plates of ambulacra. Two hydrospires per ambulacral side (see Macurda, 1962).

Peristome pentagonal, width: 1.0–1.4 mm. Some small polygonal oral cover plates known (Pl. 2, figs. 13, 14).

Remarks.– The above description is based upon the specimens in the growth series (see Appendix 1) plus RX-209 E and F (locality as for RX-209 A-D).

See SPECIES DIFFERENTIATION for a comparison between this and the other species assigned to *Schizoblastus*.

(Opposite Page)

TEXT-FIG. 2 – Growth series of *Schizoblastus marginulus* (Rowley) and *Schizoblastus moorei* Cline. See Text-figure 1 for explanation. *S. marginulus*: *C*, Lengths of RD and BR growth axes vs. deltoid length; *D*, Lengths of RD, RR, and RB growth axes vs. widths of their respective growth fronts; *E*, Triangular diagram showing percent of total radial growth of RD, RR, and RB growth axes; note poles have different values; *G*, Lengths of RD, RR, and RB growth axes vs. total growth of radial axes. *S. moorei*: *A*, Length of theca vs. width; *B*, Length of BR growth axis vs. lengths of RD and RB growth axes; *F*, Lengths of RD and RB growth axes vs. length of RR growth axis; *H*, Deltoid length vs. greatest aboral deltoid width; *I*, Ambulacral length vs. number of side plates per ambulacral side; *J*, Lengths of RD, RR, and RB growth axes vs. total growth of radial axes; *K*, Lengths of RD, RR, and RB growth axes vs. widths of their respective growth fronts; *L*, Lengths of RD and BR growth axes vs. deltoid length; *M*, Triangular diagram showing percent of total radial growth of RD, RR, and RB growth axes; note poles have different values.

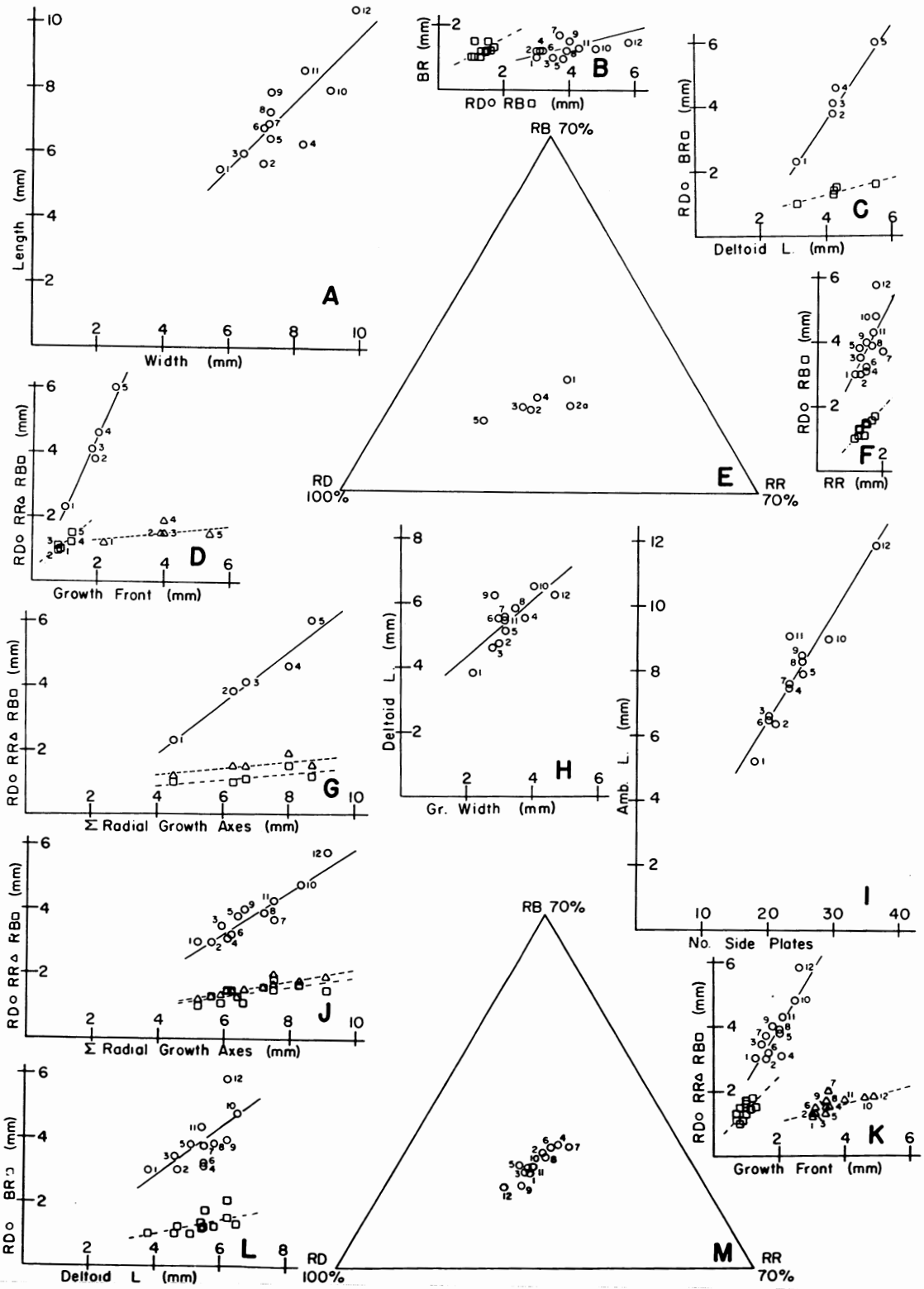
A
Length (mm)
Width (mm)
B
BR (mm)
RDo RBo (mm)
C
RDo BRo (mm)
Deltoid L. (mm)
D
RDo RRa RBo (mm)
Growth Front (mm)
E
RB 70%
RD 100%
RR 70%
F
RDo RBo (mm)
RR (mm)
G
RDo RRa RBo (mm)
Σ Radial Growth Axes (mm)
H
Deltoid L. (mm)
Gr. Width (mm)
I
Amb L. (mm)
No. Side Plates
J
RDo RRa RBo (mm)
Σ Radial Growth Axes (mm)
K
RDo RRa RBo (mm)
Growth Front (mm)
L
RDo BRo (mm)
Deltoid L (mm)
M
RB 70%
RD 100%
RR 70%

Schizoblastus moorei (Cline)

Pl. 1, figs. 1-7; Pl. 2, figs. 1-4, 8-11;

Pl. 6, fig. 2

Granatocrinus winslowi Miller and Gurley, 1894, p. 66, Pl. 6, figs. 34, 35?
Orbitremites winslowi Bather, 1899, p. 32?
Schizoblastus moorei Cline, 1936, p. 279, Pl. 45, figs. 13-16.
Schizoblastus winslowi Fay, 1961b, p. 101, Pl. 46, figs. 3-5.

Description.– Theca globose in lateral view with base being slightly protuberant to slightly recessed (Pl. 1, fig. 3; Pl. 2, fig. 2). Ambulacra long, convex, reaching almost to base of theca. Pelvis short, broad, flat to slightly convex profile, occasionally protuberant in center due to secondary deposit of calcite for stem cicatrix (Pl. 2, figs. 3, 4). Theca rounded pentagonal in plan view, with convex interambulacral areas but these are indented due to elevated ambulacra and the strong rims which border the ambulacra (Pl. 1, fig. 4; Pl. 2, fig. 1). Greatest width equatorial. Length and width subequal (text-fig. 2A; see also Table 3).

Basalia three, small, forming approximately one-half of pelvis, confined to base of theca. Outline in plan view octagonal, outline in lateral view flat to slightly convex. Configuration of area where column attaches on inner part of basalia variable. May be a simple crenellar ring 0.5 mm in diameter, or there may be a slightly raised lobose secondary deposit on the inner half of the basalia with crenellar ring in the center (Pl. 1, fig. 6; Pl. 2, fig. 3), or a strongly protuberant secondary deposit as in the holotype (Pl. 1, fig. 3; Pl. 2, fig. 4).

Azygous basal rhombic in plan view, with straight lateral edges and slightly convex distal edges. Outline in lateral view slightly convex, developing a reflexed profile if secondary deposit present. BR sector slightly convex parallel to and flat perpendicular to BR axis external to secondary deposit. Adjacent sectors merge smoothly. Zygous basals pentagonal in plan view, with straight lateral and distal lateral edges and a slightly concave distal medial edge. Lateral profile very slightly concave to slightly convex. Medial BR sector very slightly concave to very slightly convex parallel and perpendicular to BR axis if secondary deposit absent; otherwise obscured. Lateral BR sectors very slightly convex parallel to and flat perpendicular to BR axis; adjacent BR sectors merge smoothly as they do with neighboring RB sectors. Rate of growth of BR and RB axes slow, equal; that of RD and deltoid much faster (text-fig. 2B, L). ABBRF: 1.0–1.5 mm. See also Table 3.

Radials five, small; body short, limbs extending only to equator of theca. Radials pentagonal in plan view with slightly convex lower edge; lateral edges slightly convex, diverge adorally; two adoral facing edges slightly convex, slanting in toward ambulacrum. Radial quadrate in lateral view, with convex upper edge bordering ambulacrum, flat aboral facing edge, slightly concave lower edge, and slightly convex adoral facing edge. Narrow radial sinus extends nearly to base of ambulacrum. Origin of radial obscured by lip of calcite at aboral end of ambulacrum (Pl. 1, figs. 5, 6; Pl. 2, figs. 3, 4); latter bordered by prominent rim of calcite in RD sectors of radial (Pl. 1, fig. 3); upper surface of ambulacrum may be even with rims or slightly depressed below it. RB sector small, flat to very slightly convex parallel to RB axis, very slightly convex perpendicular to it. RB sectors merge over slightly convex to convex surface; merge smoothly with RR sectors. RR sector very slightly concave parallel to and convex perpendicular to RR axis; merges smoothly with RD sector. Latter convex parallel to and slightly convex perpendicular to RD axis. Radial sectors ornamented with subdued irregular nodose ornament. Rate of growth of RR and RB axes equal while that of RD is faster (text-fig. 2F); no shift in rate of growth during ontogeny (text-fig. 2J, M); rate of growth of RD is slightly less than that of deltoid (text-fig. 2L). Rate of growth of RB axis slightly faster than rate of increase of width of its growth front; RD grew much faster than the rate of increase of its growth front; converse true for RR and RRF (text-fig. 2K). See Table 3 for measurements of radial.

TABLE 3 – Growth relationships of principal variables of *Schizoblastus moorei* Cline, n = 12. See Macurda, 1966, 1967 for explanation and illustration of symbols for variables.

Variables	r	a_0	a_1	Observed range (mm) y	Observed range (mm) x
L/W	0.82	-0.76	1.06	5.5 – 10.5	5.7 – 9.7
L/Amb. L.	0.95	0.98	0.79	5.5 – 10.5	5.2 – 11.9
ABBR/RB	0.46	0.52	0.55	1.0 – 2.0	1.0 – 1.8
ABBR/RD	0.70	0.31	0.26	1.0 – 2.0	3.0 – 5.8
ABBR/Del. L.	0.62	-0.02	0.24	1.0 – 2.0	3.8 – 6.5
RD/RDF	0.82	0.56	1.73	3.0 – 5.8	1.3 – 2.6
RR/RRF	0.67	0.58	0.27	1.2 – 2.0	3.0 – 4.9
RB/RBF	0.68	0.45	1.02	1.0 – 1.8	0.7 – 1.2
RD/RR	0.62	0.69	2.04	3.0 – 5.8	1.2 – 2.0
RD/RB	0.36	2.15	1.20	3.0 – 5.8	1.0 – 1.8
RR/RB	0.86	0.33	0.86	1.2 – 2.0	1.0 – 1.8
RD/Del. L.	0.69	-0.20	0.75	3.0 – 5.8	3.8 – 6.5
RB/Del. L.	0.61	0.33	0.20	1.0 – 1.8	3.8 – 6.5
RD/Σ	0.93	-0.71	0.67	3.0 – 5.8	5.2 – 9.1
RR/Σ	0.85	0.29	0.19	1.2 – 2.0	5.2 – 9.1
RB/Σ	0.67	0.42	0.15	1.0 – 1.8	5.2 – 9.1
Del. L./Del. Gr. Ab. W.	0.76	2.48	0.88	3.8 – 6.5	2.2 – 4.7
Amb. L./No. S. P.	0.94	-0.27	0.34	5.2 – 11.9	18 – 36

r = correlation coefficient (y, x), a_0 = y intercept, a_1 = regression coefficient.

Deltoids four, together with epideltoid forming border to peristome. Deltoid triangular in plan view, occupying one-half of length of theca, convex in lateral view, concave in cross section due to prominent rims on edge of deltoid body bordering ambulacrum (Pl. 1, fig. 2). Adoral edge of deltoid bordering peristome straight; width expands along short straight DDF; width contracts along suture with lancet and side plates to narrowest part of plate at spiracles; width of deltoid body then expands aborally along straight suture with side plates; greatest width of plate at radiodeltoid suture with each half of suture being slightly concave. Central part of deltoid lip triangular, elevated; adoral faces bear minor grooves of ambulacral tract. Elevated area on deltoid lip continues between spiracles, then rises into a massive elevated surface (Pl. 1, fig. 2). Aborally this surface divides into two ridges which form edge to deltoid body and form a rim to the ambulacrum which is depressed below it. Top of rim ornamented by a single (occasionally double) line of nodes. Interior of deltoid body at lower elevation than rims, convex in cross section, ornamented by a few median nodes; very broad growth lines occasionally visible (Pl. 1, fig. 7). Rarely, nodes may be developed lateral to the medial nodes (Pl. 1, fig. 3). Radial extends adorally beneath deltoid along margins of ambulacrum as in

S. sayi. Length of deltoid increases more rapidly ontogenetically than the width of the plate (text-fig. 2H; see also Table 3).

Anal deltoids two, an epi- and hypodeltoid (Pl. 1, fig. 2). Outline of epideltoid as for deltoid lip of regular deltoid; aboral edge embayed by anal opening. Upper surface forms massive horseshoe-shaped collar to adoral half of anal opening. Outline and ornament of hypodeltoid (Pl. 1, fig. 1) as for deltoid body of regular deltoid except adoral end which is embayed by aboral half of anal opening and elevated to form a hood to the anal opening. Anal opening (L: 0.4–0.8 mm; W.: 0.3–0.7 mm) ovoid, bordered adorally by epideltoid, aborally by hypodeltoid; area increases ontogenetically (text-fig. 5F).

Ambulacra five, linear, relatively narrow, extending from near peristome almost to base of theca. Ambulacra convex in lateral view and in cross section except for depression along median for ambulacral tract. Upper surface of aboral half of ambulacrum even with or slightly elevated above level of surrounding radial rim while adorally upper surface is depressed below bordering rims of the deltoid. Lancet narrowly exposed from slightly over one-half to two-thirds of the ambulacral length. Lancet rhombic in cross section where covered by side plates, pentagonal where exposed; here upper surface bears part of ambulacral tract. Overall shape of side plates triangular, with slightly convex admedial edge, straight adoral and aboral edges; short edge abuts against radial or deltoid. Large triangular outer side plate wedges inward between side plates; outer edge borders radial or deltoid. Small triangular hydrospire pores present along border of ambulacrum with radial, absent along deltoid due to continued lateral growth of side and outer side plates. Hydrospire pore bordered laterally by radial, adorally by side plate, aborally by outer side plate; arcuate pore furrow leads into it. Brachiolar facet on outer sloping side of ambulacrum, equally developed on side and outer side plates, length 0.2 mm, width 0.15 mm (Pl. 6, fig. 2). Three or four minor grooves border main groove per side plate; also three or four minor grooves border adoral and aboral margins of side groove. Approximately three side plates per mm (text-fig. 2I); number of brachioles increases as size of viscera increases (text-fig. 5D). Amb. L.: 5.2–11.9 mm; Amb. W.: 1.0–1.5 mm; No. S. P.: 18–36. See also Table 3.

Ten spiracles, those in anal interarea distinctly separated from anal opening. Regular spiracles set approximately 0.5 mm apart (on same deltoid) and adoral ends are approximately 1.0 mm from center of peristome. Spiracle teardrop-shaped (0.3 by 0.2 mm), bordered adorally and on inner side by deltoid, on outer side by side plates. Anal spiracles similar shape, bordered adorally by epideltoid, on inner side by hypodeltoid, and on outer side by side plates; set farther from center of peristome because of larger size of epideltoid. Ten groups of hydrospires, with two hydrospires per group including anal interarea (USNM 248322). Hydrospire pores present along radial, absent along deltoid.

Peristome pentagonal, width 0.3–0.5 mm.

Remarks.– The above description is based upon the specimens in the growth series, plus one additional sectioned specimen (USNM 160697) from the St. Joe Formation at Eureka Springs, Arkansas. Cline (1936, p. 280) listed two paratypes for *S. moorei*. The squatter, more ovoid of these is a specimen of *S. sayi*.

(Opposite Page)

TEXT-FIG. 3 – Growth series of *Schizoblastus aplatus* (Rowley and Hare) and *Schizoblastus sayi* (Shumard). *S. sayi* is growth series A unless otherwise indicated. See Text-figure 1 for explanation. *S. aplatus*: *D*, Total number of brachioles per specimen vs. volume of viscera. *S. sayi*: *A*, Ambulacral length vs. number of side plates per ambulacral side; H = holotype of *S. sayi*; HP = holotype of *Pentremites potteri* Hambach; *B*, Length of thecae in five growth series vs. width; dashed line, growth series A (Burlington, Ia.); solid line, growth series B (Hannibal, Mo.); dash-dot, dot line, growth series C (Reeds Spring, Mo.); dash-dot line, growth series D (Central Mo.); dotted line, growth series E (Louisiana, Mo.); *C*, Length of BR growth axis vs. lengths of RD and RB growth axes; *E*, Lengths of RD, RR, and RB growth axes vs. total growth of radial axes; *F*, Lengths of RD and BR growth axes vs. deltoid length; *G*, Lengths of RD and RB growth axes vs. length of RR growth axis.

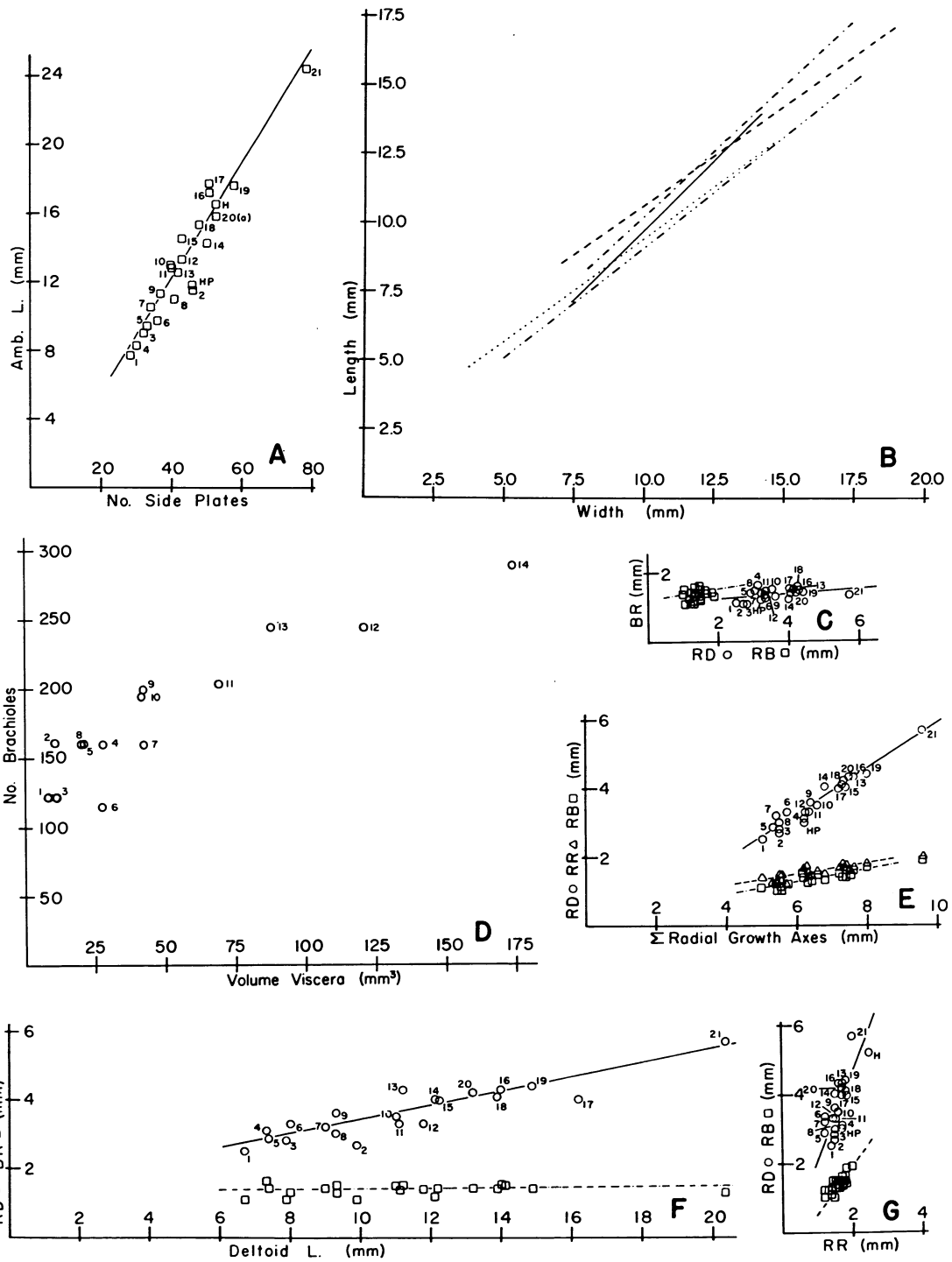
Amb. L. (mm)
No. Side Plates
A
Length (mm)
Width (mm)
B
No. Brachioles
Volume Viscera (mm³)
D
BR (mm)
RD○ RB□ (mm)
C
RD○ RR△ RB□ (mm)
Σ Radial Growth Axes (mm)
E
RD○ BR□ (mm)
Deltoid L. (mm)
F
RD○ RB□ (mm)
RR (mm)
G

Miller and Gurley (1894) described the species *Granatocrinus winslowi* from the Burlington Ls.?, drift at Danville, Illinois. The holotype, which is silicified (Pl. 2, figs. 5-7), resembles *S. moorei* in its morphology but the upper part of the anal interarea has been weathered away. Although suggestive of being a senior synonym of *S. moorei, Granatocrinus winslowi* is herein considered a *nomina dubia* because of the imperfect preservation. The bedrock near Danville, Illinois is Pennsylvanian in age and the source of this specimen is uncertain. This uncertainty is compounded by a specimen in the U.S. National Museum (Pl. 2, figs. 9-11) which is an *S. moorei*; its locality is given as "drift, Danville, Illinois."

See SPECIES DIFFERENTIATION for a comparison between this and the other species assigned to *Schizoblastus.*

Schizoblastus sayi (Shumard, 1855)

Pl. 1, figs. 9, 12, 13; Pl. 3, figs. 1, 2, 7, 12-14;

Pl. 4, figs. 1-19; Pl. 5, figs. 1-8, 10-12;

Pl. 6, figs. 4-6

Pentremites sayi Shumard, 1855, p. 185, Pl. B, figs. 1a-d.
Granatocrinus sayi Shumard, 1866, p. 376.
Pentremites potteri Hambach, 1880, p. 156, Pl. B, fig. 4.
Schizoblastus sayi Etheridge and Carpenter, 1882, p. 246.
Schizoblastus potteri Etheridge and Carpenter, 1882, p. 247.
Cribroblastus potteri Hambach, 1903, p. 41, Pl. 5, fig. 15.
Cribroblastus sayi Hambach, 1903, p. 42, Pl. 5, fig. 14.
Cribroblastus verrucosus Hambach, 1903, p. 58, Pl. 5, fig. 3.
Schizoblastus ? verrucosus Bather, 1908, p. 318.
Schizoblastus sayi Cline, 1936, p. 266.
Schizoblastus sayi var. *sayi* Cline, 1936, p. 269, Pl. 44, figs. 17-22.
Schizoblastus sayi var. *bellulus* Cline, 1936, p. 271, Pl. 45, figs. 1-8.
Schizoblastus sayi var. *obesus* Cline, 1936, p. 272, Pl. 44, figs. 6-16.
Schizoblastus sayi var. *potteri* Cline, 1936, p. 272, Pl. 45, figs. 21-25.
Schizoblastus sayi var. *verrucosus* Cline, 1936, p. 274, Pl. 45, fig. 12.
Schizoblastus laudoni Cline, 1936, p. 277, Pl. 44, figs. 1-5.
Schizoblastus burlingtonensis Cline, 1936, p. 280, Pl. 45, figs. 9-11.

Description.– Theca ellipsoidal to globose; length usually slightly greater than width but reverse true as well (text-fig. 3B). Ambulacra convex, very elongate, reaching to base of theca (Pl. 4, figs. 2, 5, 8, 9, 11) so pelvis (diameter: 4.4–6.6 mm) confined to very base of theca (Pl. 4, figs. 3, 6, 13). Greatest width equatorial. Outline in plan view circular (Pl. 4, figs. 1, 4, 7, 10), with narrow convex ambulacra and wide, convex interambulacral areas. Length usually 15 mm or less, but a few larger specimens occasionally found (see Table 4).

Basalia three, in normal position, confined to base of theca, forming about one-half of pelvis (Pl. 1, figs. 9, 12, 13). In plan view outline of basals pentagonal, with slightly concave edges against C and E radials, and straight but broadly V-shaped sutures against other radials. Most of basals usually covered by cylindrical, short, massive secondary deposit of calcite which bears columnal cicatrix; sides of secondary deposit usually have warty or coarse frilly pattern (Pl. 1, figs. 12, 13); columnal cicatrix on slightly recessed lower center of deposit; crenellar lobes and facets at edge of columnal cicatrix; diameter of column (0.7–1.0 mm) relatively small in relation to secondary deposit of calcite (1.7–2.7 mm). Secondary deposit usually just visible in lateral view; its degree of development is variable, however, and occasionally columnal cicatrix can be a simple depression in center of basals

TABLE 4 – Growth relationships of principal variables of *Schizoblastus sayi* (Shumard), growth series A–E. A: n = 21 except first, second and last equation where n = 22; B: n = 15; C: n = 17; D: n = 11; E: n = 15. See Macurda, 1966, 1967 for explanation and illustration of symbols for variables.

Variables		r	a_o	a_1	Observed range (mm) y	Observed range (mm) x
L/W	A	0.87	3.47	0.73	7.4 – 17.0	7.0 – 19.6
	B	0.92	-0.35	1.00	7.2 – 15.0	7.5 – 13.8
	C	0.97	1.03	0.80	5.5 – 14.7	6.0 – 17.5
	D	0.78	0.76	0.96	8.5 – 19.0	8.0 – 17.0
	E	0.94	1.22	0.80	5.0 – 13.3	5.0 – 14.2
L/Amb. L.	A	0.95	2.41	0.67	7.4 – 17.0	7.7 – 24.4
	B	0.97	1.04	0.77	7.2 – 15.0	8.0 – 16.8
	C	0.97	1.83	0.66	5.5 – 14.7	5.7 – 19.5
	D	0.94	0.57	0.84	8.5 – 19.0	8.8 – 19.8
	E	0.96	2.28	0.59	5.0 – 13.3	5.0 – 17.0
ABBR/RB	A	0.24	1.15	0.15	1.1 – 1.6	1.0 – 1.9
	B	0.30	0.88	0.21	1.0 – 1.7	1.5 – 2.5
	C	0.89	0.47	0.44	1.0 – 1.7	1.2 – 2.6
	D	0.78	0.39	0.54	0.9 – 1.6	1.0 – 2.2
	E	0.44	0.58	0.48	1.1 – 2.0	1.2 – 2.0
ABBR/RD	A	0.33	1.13	0.07	1.1 – 1.6	2.5 – 5.7
	B	0.17	1.06	0.05	1.0 – 1.7	3.1 – 5.7
	C	0.77	0.71	0.13	1.0 – 1.7	2.5 – 7.3
	D	0.66	0.56	0.18	0.9 – 1.6	3.0 – 5.7
	E	0.12	1.20	0.04	1.1 – 2.0	2.2 – 5.0
ABBR/Del. L.	A	0.21	1.30	0.01	1.1 – 1.6	6.7 – 20.4
	B	0.58	0.79	0.05	1.0 – 1.7	6.8 – 14.8
	C	0.81	0.78	0.05	1.0 – 1.7	4.8 – 17.0
	D	0.87	0.66	0.05	0.9 – 1.6	7.9 – 18.3
	E	0.19	1.20	0.01	1.1 – 2.0	3.9 – 15.0
RD/RDF	A	0.83	0.91	1.20	2.5 – 5.7	1.5 – 3.6
	B	0.69	1.27	1.14	3.1 – 5.7	1.7 – 3.2
	C	0.93	0.42	1.51	2.5 – 7.3	1.2 – 4.0
	D	0.86	1.26	1.05	3.0 – 5.7	1.7 – 3.8
RR/RRF	A	0.75	0.86	0.21	1.2 – 2.0	2.2 – 5.3
	B	0.74	0.52	0.38	1.5 – 2.7	2.7 – 4.9
	C	0.85	0.67	0.29	1.0 – 2.5	2.2 – 5.8
	D	0.60	0.20	0.42	1.1 – 2.4	2.7 – 4.5

TABLE 4 – Cont'd.

Variables		r	a_o	a_1	Observed range (mm) y	Observed range (mm) x
RB/RBF	A	0.50	0.47	0.91	1.0 – 1.9	0.8 – 1.3
	B	0.20	1.57	0.33	1.5 – 2.4	0.7 – 1.4
	C	0.73	0.12	1.68	1.2 – 2.6	0.7 – 1.5
	D	0.70	-0.57	2.15	1.0 – 2.2	0.9 – 1.2
RD/RR	A	0.71	-0.42	2.55	2.5 – 5.7	1.2 – 2.0
	B	0.68	1.33	1.47	3.1 – 5.7	1.5 – 2.7
	C	0.88	-1.46	3.21	2.5 – 7.3	1.0 – 2.5
	D	0.68	1.69	1.35	3.0 – 5.7	1.1 – 2.4
	E	0.60	0.41	1.96	2.2 – 5.0	1.4 – 2.3
RD/RB	A	0.75	0.19	2.44	2.5 – 5.7	1.0 – 1.9
	B	0.75	0.72	1.78	3.1 – 5.7	1.5 – 2.4
	C	0.84	-0.22	2.52	2.5 – 7.3	1.2 – 2.6
	D	0.38	2.42	0.96	3.0 – 5.7	1.0 – 2.2
	E	0.61	0.26	2.27	2.2 – 5.0	1.2 – 2.0
RR/RB	A	0.81	0.55	0.74	1.2 – 2.0	1.0 – 1.9
	B	0.82	0.18	0.90	1.5 – 2.7	1.5 – 2.4
	C	0.86	0.53	0.70	1.0 – 2.5	1.2 – 2.6
	D	0.78	0.07	1.01	1.1 – 2.4	1.0 – 2.2
	E	0.56	0.74	0.64	1.4 – 2.3	1.2 – 2.0
RD/Del. L.	A	0.87	1.37	0.20	2.5 – 5.7	6.7 – 20.4
	B	0.72	2.05	0.20	3.1 – 5.7	6.8 – 14.8
	C	0.90	1.06	0.30	2.5 – 7.3	4.8 – 17.0
	D	0.71	2.15	0.15	3.0 – 5.7	7.9 – 18.3
	E	0.90	1.62	0.24	2.2 – 5.0	3.9 – 15.0
RB/Del. L.	A	0.78	0.78	0.05	1.0 – 1.9	6.7 – 20.4
	B	0.83	0.91	0.09	1.5 – 2.5	6.8 – 14.8
	C	0.93	0.67	0.10	1.2 – 2.6	4.8 – 17.0
	D	0.82	0.81	0.07	1.0 – 2.2	7.9 – 18.3
	E	0.54	1.22	0.04	1.2 – 2.0	3.9 – 15.0
RD/Σ	A	0.97	-0.65	0.65	2.5 – 5.7	5.0 – 9.6
	B	0.95	-0.21	0.55	3.1 – 5.7	6.5 – 10.4
	C	0.99	-0.71	0.64	2.5 – 7.3	4.7 – 12.3
	D	0.91	-0.07	0.55	3.0 – 5.7	6.1 – 9.9
	E	0.96	-1.09	0.69	2.2 – 5.0	4.8 – 9.0

TABLE 4 – Cont'd.

Variables		r	a_o	a_1	Observed range (mm) y	Observed range (mm) x
RR/Σ	A	0.86	0.50	0.16	1.2 – 2.0	5.0 – 9.6
	B	0.86	0.05	0.23	1.5 – 2.7	6.5 – 10.4
	C	0.93	0.48	0.17	1.0 – 2.5	4.7 – 12.3
	D	0.91	-0.32	0.28	1.1 – 2.4	6.1 – 9.9
	E	0.76	0.57	0.17	1.4 – 2.3	4.8 – 9.0
RB/Σ	A	0.89	0.17	0.18	1.0 – 1.9	5.0 – 9.6
	B	0.90	0.16	0.22	1.5 – 2.5	6.5 – 10.4
	C	0.91	0.23	0.20	1.2 – 2.6	4.7 – 12.3
	D	0.71	0.39	0.17	1.0 – 2.2	6.1 – 9.9
	E	0.76	0.53	0.15	1.2 – 2.0	4.8 – 9.0
Del. L./Del. Gr. Ab. W.	A	0.95	-1.00	2.79	6.7 – 20.4	3.0 – 7.5
	B	0.94	-0.55	2.21	6.8 – 14.8	3.6 – 6.8
	C	0.99	-1.23	2.43	4.8 – 17.0	2.6 – 7.8
	D	0.98	-0.67	2.41	7.9 – 18.3	3.8 – 8.2
Amb. L./No. S. P.	A	0.96	-1.35	0.33	7.7 – 24.4	28 – 79
	B	0.96	-2.49	0.39	8.0 – 16.8	28 – 48
	C	0.97	-4.99	0.48	5.7 – 19.5	23 – 49
	D	0.97	-1.90	0.37	8.8 – 19.8	30 – 54
	E	1.00	0.21	0.32	5.0 – 17.0	15 – 53

r = correlation coefficient (y, x), a_o = y intercept, a_1 = regression coefficient.

with no secondary deposit of calcite (Pl. 1, fig. 9); in this instance, basals not visible in lateral view and base is very slightly concave. Secondary deposit circular, usually covers most of basals, extending out to radial-basal suture along interbasal suture. (Compare Pl. 1, figs. 9, 12, 13.) Small lumen pierces proximal junction of three basals. Azygous basal rhombic, with almost straight interbasal sutures and slightly convex radial-basal sutures; that portion not covered by secondary calcite slightly convex both in length and width, slightly more pronounced normal to BR axis in each BR sector; ornamented by growth lines parallel to radial-basal sutures. Zygous basals pentagonal, with straight lateral and distal lateral sutures; slightly concave distal medial edge. That portion not covered by secondary calcite slightly convex in length and width; convexity slightly more pronounced normal to BR axis in medial RR sector. Ornament as for azygous basal. Rate of growth of BR and RB axes nearly equal while RD axis and deltoid have much higher rate of growth than BR axis (text-fig. 3C,F; Table 4). ABL: 1.3–2.0 mm; ABW: 1.5–2.3 mm; ABBB: 0.7–1.5 mm; ABBRF: 1.1–1.8 mm.

Radials five, confined externally to lower one-quarter of theca, but extending well adorally beneath ambulacra as hydrospires (Pl. 3, fig. 7). Outline in plan view short, broad, hexagonal (Pl. 5, fig. 10), with slightly convex (C and E radials) or broad V-shaped radial-basal edge (A, B, and D

radials); lateral edges slightly convex, expanding in width up to deltoid; edge against deltoid convex, edge near ambulacrum reaching farther adorally than edge near interradial suture. Deep, narrow U-shaped radial sinus reaches almost to base of plate. In lateral view radial is convex parallel to ambulacrum; aboral face concave; interradial suture slightly concave. Radial convex in cross section with raised lip parallel to ambulacrum, elevating ambulacrum above surrounding plates. Origin of radial covered by a small lip of calcite at aboral end of ambulacrum (Pl. 1, fig. 9). RB sector small, confined to base of calyx; RB sector is straight parallel to RB axis and slightly convex normal to it; two adjacent sectors merge over straight to slightly convex boundary; RB sectors curve smoothly into RR sectors. Latter are slightly concave (produced in part by radial lip) to flat parallel to RR axis, convex normal to it; curve smoothly into RD sectors. RD sector is largest of three, growth being most rapid in this direction (text-figs. 3E, 4C; Table 4); sector convex parallel to RD axis, almost flat normal to it except for raised rim parallel to ambulacrum (Pl. 5, fig. 4). Growth rates of RR and RB axes nearly equal to one another (text-fig. 3G); no shift in relative growth rates of axes observed (text-fig. 4E). RD has fastest rate of growth relative to width of its growth front while RR has the widest growth front (text-fig. 4B). Growth rate of RD less than that of deltoid (text-figs. 3F, 4A; Table 4). Ornament of radial comprised of fairly strong growth lines parallel to sutures, crowded in RB sector, fanning out in RR sector (Pl. 5, fig. 10), due to faster rate of growth in RD sector. Growth lines are not seen on ambulacral rim which apparently represents a slight secondary deposit on surface of plate; this becomes more pronounced toward radiodeltoid suture.

Deltoids four, together with epideltoid form border to peristome. Deltoids very large, extending three-fourths length of theca and overlapping radial (Pl. 3, figs. 1, 7). Adoral tip of deltoid (deltoid lip) small (Pl. 4, figs. 1, 4, 7, 18), quadrate-hexagonal with edge bordering peristome straight to very slightly concave; DDF straight, short, diverge aborally; bear main ambulacral groove which is bordered by minor grooves; DAF short, straight, subparallel, extending to spiracle. Upper surface of deltoid lip bears prominent adorally directed V-shaped rim which borders ambulacrum (Pl. 4, fig. 18). Deltoid constricts around spiracles (0.5–1.3 mm wide); here rim swings away from ambulacrum, being concave around spiracle; upper edge sharp; two rims of deltoid diverge and die out aborally (Pl. 5, fig. 5). Small, arrowhead-shaped depression in adoral center of deltoid surrounded by rim of deltoid (Pl. 4, fig. 18). Aboral body of deltoid large, triangular-shaped in plan view (Pl. 5, fig. 2), with convex suture against ambulacrum, and gull winged shaped suture against radials (Pl. 5, fig. 1), convex through more than 90° in lateral view; in cross section overall profile convex but there are two slightly concave areas marginal to medial ridge. In small and medium sized specimens, width of deltoid is equal at equator of theca and radiodeltoid suture, but in large specimens greatest width is equatorial. Deltoid is massive in appearance and may form overhang above radials (Pl. 4, fig. 14). Ornament of deltoid body comprised of median ridge which arises in adoral part of body and extends to interradial suture; may bear various nodes (Pl. 3, fig. 2; Pl. 4, figs. 8, 9; Pl. 5, figs. 1, 2); laterally, there are two relatively flat areas (very rarely, ornamented with columns of nodes); there are two broad, massive rims marking continuation of adoral rim of deltoid along lateral borders of deltoid (Pl. 3, figs. 1, 12; Pl. 4, figs. 11, 19; Pl. 5, figs. 1, 2); these diverge aborally and extend to lateral edges of radiodeltoid suture and are continuous with the rim bordering the ambulacrum on the radial (becoming sharper and narrower here; Pl. 5, fig. 1); lateral rises may bear nodes. Deltoid grows by addition of calcite on radiodeltoid suture and by the lateral addition of calcite parallel to the ambulacrum (Pl. 4, figs. 2, 5, 8, 9, 11). Growth lines paralleling radiodeltoid suture (Pl. 4, fig. 12) and ambulacra are usually massive; former may be ornamented with nodes; in larger specimens those paralleling ambulacra are usually broadest near equator of specimen and taper slightly aborally; adorally, they converge toward a common point aboral or just marginal to spiracle. That portion of deltoid body formed by lateral growth becomes increasingly prominent with age; it is triangular-

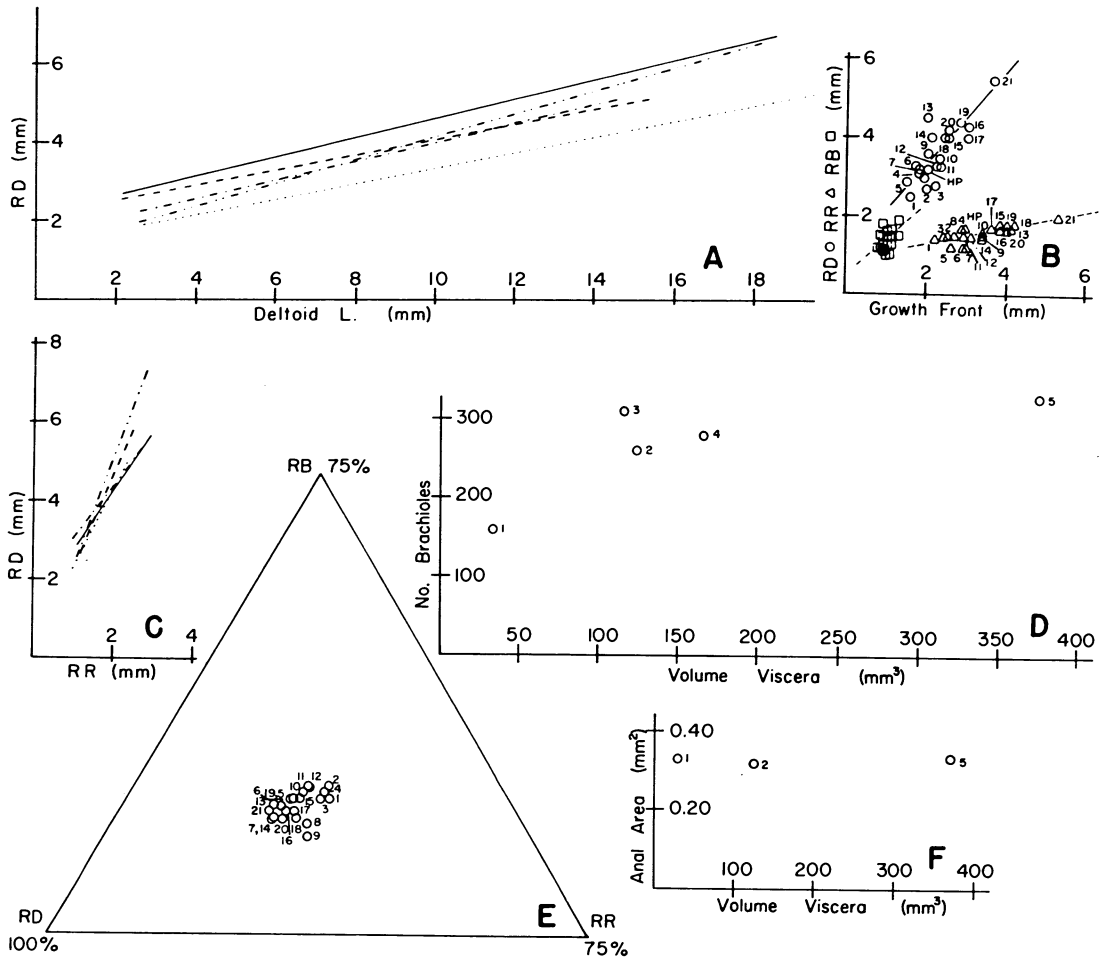

TEXT-FIG. 4 – Growth series of *Schizoblastus marginulus* (Rowley) and *Schizoblastus sayi* Shumard. See Text-figures 1 and 3 for explanation. *S. marginulus*: *D*, Total number of brachioles per specimen vs. volume of viscera; *F*, Area of anal opening vs. volume of viscera. *S. sayi*: *A*, Length of RD growth axes in five growth series vs. deltoid lengths; *B*, Length of RD, RR, and RB growth axes vs. lengths of their respective growth fronts; *C*, Length of RD growth axes in five growth series vs. length of RR growth axes; *E*, Triangular diagram showing percent of total radial growth of RD, RR, and RB growth axes; note poles have different volumes.

shaped because of the growth relationships of the deltoid. The deltoid length, when measured in an arc, is considerably greater than deltoid width (text-fig. 5B). Other growth relationships of the deltoid are given in text-figures 3F, 4A, and Table 4.

Anal deltoids two, an epi- and hypodeltoid. Outline of epideltoid as for regular deltoid, except aboral edge embayed by anus; adorally, there is a massive triangular rim which rises above the peri-

stome and projects partly over it (Pl. 4, fig. 4; Pl. 5, fig. 11). No depression on epideltoid as in corresponding position on regular deltoid. Externally, epideltoid forms adoral border of anal interarea spiracles; epi-hypodeltoid suture at right angle to center of anus. Epideltoid continues internally to form hydrospires. Except for adoral tip, configuration and ornament of hypodeltoid as for body of regular deltoid. Adoral tip of hypodeltoid embayed for anal opening; plate rises above anus to form a hood almost at right angles to surface of epideltoid (Pl. 5, fig. 11). Lateral growth increments of hypodeltoid converge on each aboral lateral side of this hood. Anal opening circular, plane of opening being above peristome; axis slopes down and away from oral surface. Anal opening L: 0.5–1.0 mm; W: 0.4–0.9 mm. Small angular plates form an anal chimney (Pl. 5, fig. 12); lowermost plates fit into the right angle of the epi- and hypodeltoid hood which is faceted (Pl. 5, fig. 11); maximum height unknown (anal chimney best known from one specimen figured but base plates of chimney known from several other specimens from different localities); plates of anal chimney not connected to those covering peristome. Size of anal opening increases as the volume of the viscera increases (text-fig. 5E). O.c.–anus: 0.6–2.0 mm.

Ambulacra five, linear, narrow, elongate, reaching to very base of theca (Pl. 5, fig. 4). Ambulacrum convex in cross section with sloping sides; concave median trough sloping down to main ambulacral groove. Upper surface of ambulacrum usually even with rim of deltoid and elevated above radial. Lower edge of side of ambulacrum meets deltoid in shallow V-shaped trough; edge set very slightly below rim on radial. Hypodeltoid hood rises strongly above ambulacrum. In lateral view ambulacrum is convex through almost 180° in large specimens (Pl. 4, figs. 11, 14). Lancet closely approaches peristome; outline in plan and lateral view that of ambulacrum; exposed along main ambulacral groove and lateral to this (along part of area of minor grooves and lobes; Pl. 5, fig. 6) almost to aboral tip of ambulacrum. In aboral part of ambulacrum lancet has V-shaped depression at top for main ambulacral groove; sides slope steeply down, slightly sinusoidal where side plates abut against it; maximum width at lowermost internal extremities of side plates; lower edge of lancet convex. In adoral part this lower edge of lancet becomes sharply concave. Lancet increases in width and height from aboral end to point near peristome, aboral to spiracles. At its aboral end, lancet rests upon trough in solid calcite of radial (Pl. 5, fig. 3) (for 4 mm in a specimen 18 mm in length); adoral to this it is exposed in the interior of the theca, being in contact on its bottom lateral edge with the upper, more thickly calcified (0.1 mm) inner wall of the hydrospire groups. Adoral tip abuts against two deltoids which very slightly overlap adoralmost tip of lancet. At adoral end entire bottom surface of lancet exposed to interior; aborally after passing spiracles, it is supported on the lateral bottom by the inner, more calcified wall of the hydrospires formed by the deltoids, analogous to that of the radial; these extend aborally to meet those of the radial; those of radial underlie slightly

---

(Opposite Page)

TEXT-FIG. 5 – Growth series of *Schizoblastus aplatus* (Rowley and Hare), *Schizoblastus moorei* Cline, and *Schizoblastus sayi* (Shumard). See Text-figures 1 and 3 for explanation. *S. aplatus: C,* Area of anal opening vs. volume of viscera. *S. moorei: D,* Total number of brachioles per specimen vs. volume of viscera; *F,* Area of anal opening vs. volume of viscera. *S. sayi: A,* Total number of brachioles per specimen vs. volume of viscera; *B,* Deltoid lengths in five growth series vs. maximum aboral deltoid widths; *E,* Area of anal opening vs. volume of viscera.

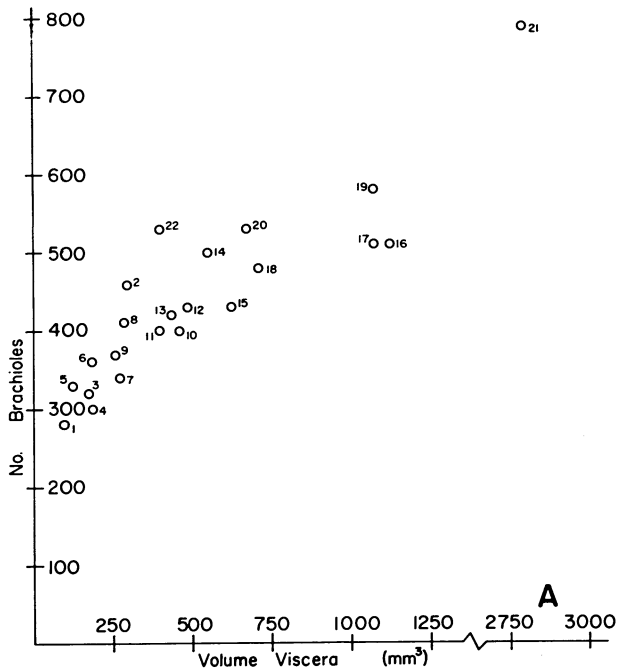
No. Brachioles
800
700
600
500
400
300
200
100
250 500 750 1000 1250 2750 3000
Volume Viscera (mm³)
A

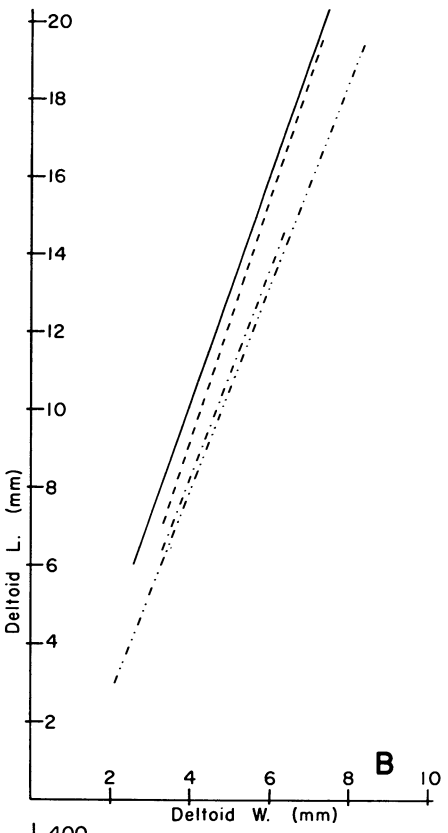
Deltoid L. (mm)
20
18
16
14
12
10
8
6
4
2
2 4 6 8 10
Deltoid W. (mm)
B

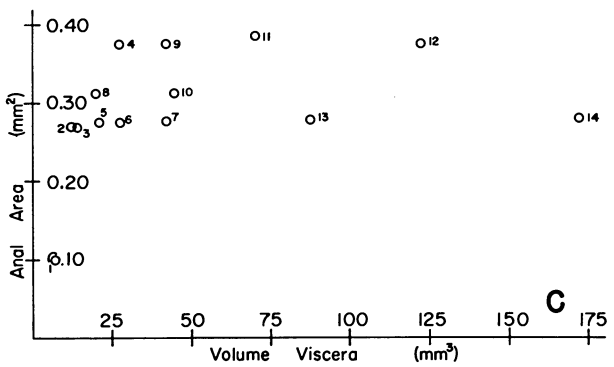
Anal Area (mm²)
0.40
0.30
0.20
0.10
25 50 75 100 125 150 175
Volume Viscera (mm³)
C

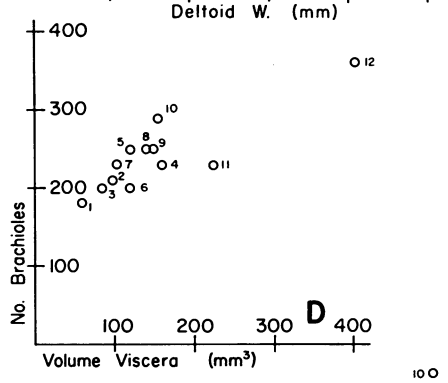
No. Brachioles
400
300
200
100
100 200 300 400
Volume Viscera (mm³)
D

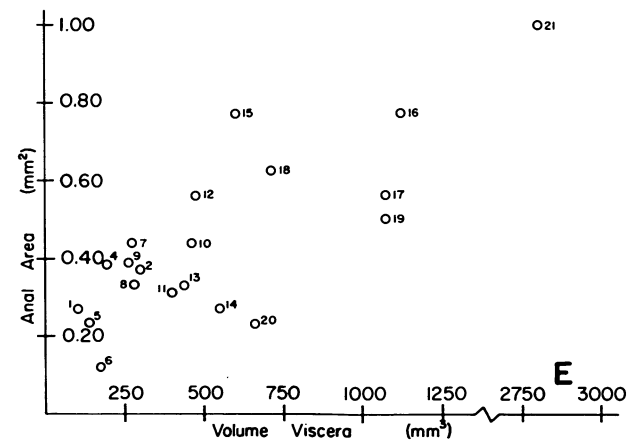
Anal Area (mm²)
1.00
0.80
0.60
0.40
0.20
250 500 750 1000 1250 2750 3000
Volume Viscera (mm³)
E

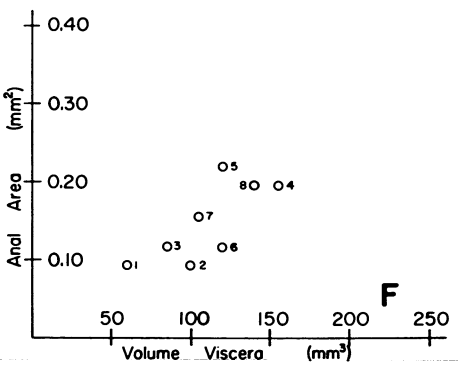
Anal Area (mm²)
0.40
0.30
0.20
0.10
50 100 150 200 250
Volume Viscera (mm³)
F

more than three-fourths of ambulacral length. (The aboral part of this calcified support on the radial would have been called an "underlancet plate" by earlier workers but it is part of the radial, being optically continuous with it.) Lancet canal pierces lancet slightly above center.

In the aboral part of the ambulacrum, the side plates have a quadrate inner half and triangular outer half in plan view, being slightly convex against the lancet; sutures with adjacent side plates straight, directed somewhat aborally. Adoral suture with abmedial elongate, triangular outer side plate very slightly concave; side plate embayed aborally by triangular pore and outer side plate; tapering adoral half bears aboral part of an ellipsoidal, admedially embayed brachiolar facet, while outer side plate bears adoral half (Pl. 6, figs. 4, 6). Hydrospire pore bordered adorally by side plate, aborally by outer side plate, and laterally by radial or aboral part of deltoid (Pl. 6, figs. 4, 6); outer side plate and side plate in contact with radial. Pores become nonfunctional adorally during growth; side plate continues to grow laterally, filling up the pore and completely surrounding the outer side plate (Pl. 5, fig. 6; Pl. 6, figs. 5, 6); Amb. W.: 1.0–2.2 mm. This is most pronounced near the middle of the deltoid. Brachiolar facets on outer sloping side of side plates and outer side plates; short ambulacral side groove connects it to main ambulacral groove. Main ambulacral groove and aboral part of side ambulacral groove bordered by minor grooves and lobes. Highest part of ambulacral profile occurs on side plates between brachiolar facets and minor grooves and lobes bordering main ambulacral groove. Internally, side plate is wedge-shaped with slightly sinusoidal suture against lancet, straight against deltoid (or radial). Outer side plate underlain by side plates. The number of side plates increases uniformly during the growth of an individual (text-fig. 3A; Table 4); the addition of new brachioles keeps pace with the volumetric expansion of the viscera (text-fig. 5A).

Spiracles ten, teardrop-shaped; those in anal interarea separated from anal opening, causing embayment in sides of hypodeltoid. Adoral and inner lateral border formed by deltoid (or epi- and hypodeltoid); outer lateral border by side plates of ambulacrum; lead internally to ten hydrospire groups with two hydrospires per group; hydrospires begin just aboral to spiracle, adoral approximately one-fourth of which formed by deltoid, remainder from radials. Hydrospire canal visible in interior of theca, quadrate in cross section, higher than wide (visible with side plates and lancet removed as a band of clear calcite between solid plate and more highly calcified inner wall of hydrospires), bounded laterally by upper hydrospire walls; thickness of these walls increases toward theca and lancet. Two pendant hydrospires hang below with thin parallel upper walls and a bulbous lower sac. Number apparently invariant with size or locality. O.c.–spir.: 0.9–2.0 mm; Spir. L.: 0.5–1.1 mm; W.: 0.1–0.3 mm.

Peristome rounded pentagonal, wider than high, with concave faces produced by deltoid and epideltoid lips; Peris. W.: 0.9–2.5 mm. Peristome roofed over by polygonal cover plates (Pl. 5, figs. 5, 11) which are not uncommon; these continue over main ambulacral groove on deltoids as a double (or rarely quadruple) row of plates, producing a circular tunnel, presumably extended over the rest of the ambulacral system. Brachioles unknown.

Pentagonal ring canal around peristome, connecting with lancet canals on internal mold (Pl. 5, fig. 7).

One four-fold mutant known (Pl. 5, fig. 8).

(Opposite Page)

TEXT-FIG. 6 – Growth series of *Decemoblastus melonoides* (Meek and Worthen). See Text-figure 1 for explanation. *A*, Lengths of RD, RR, and RB growth axes vs. total growth of radial axes; *B*, Lengths of RD and RB growth axes vs. length of RR growth axis; *C*, Lengths of RD and RR growth axes vs. deltoid length; *D*, Lengths of RD, RR, and RB growth axes vs. lengths of their respective growth fronts; *E*, Area of anal opening vs. volume of viscera; *F*, Length of theca vs. width.

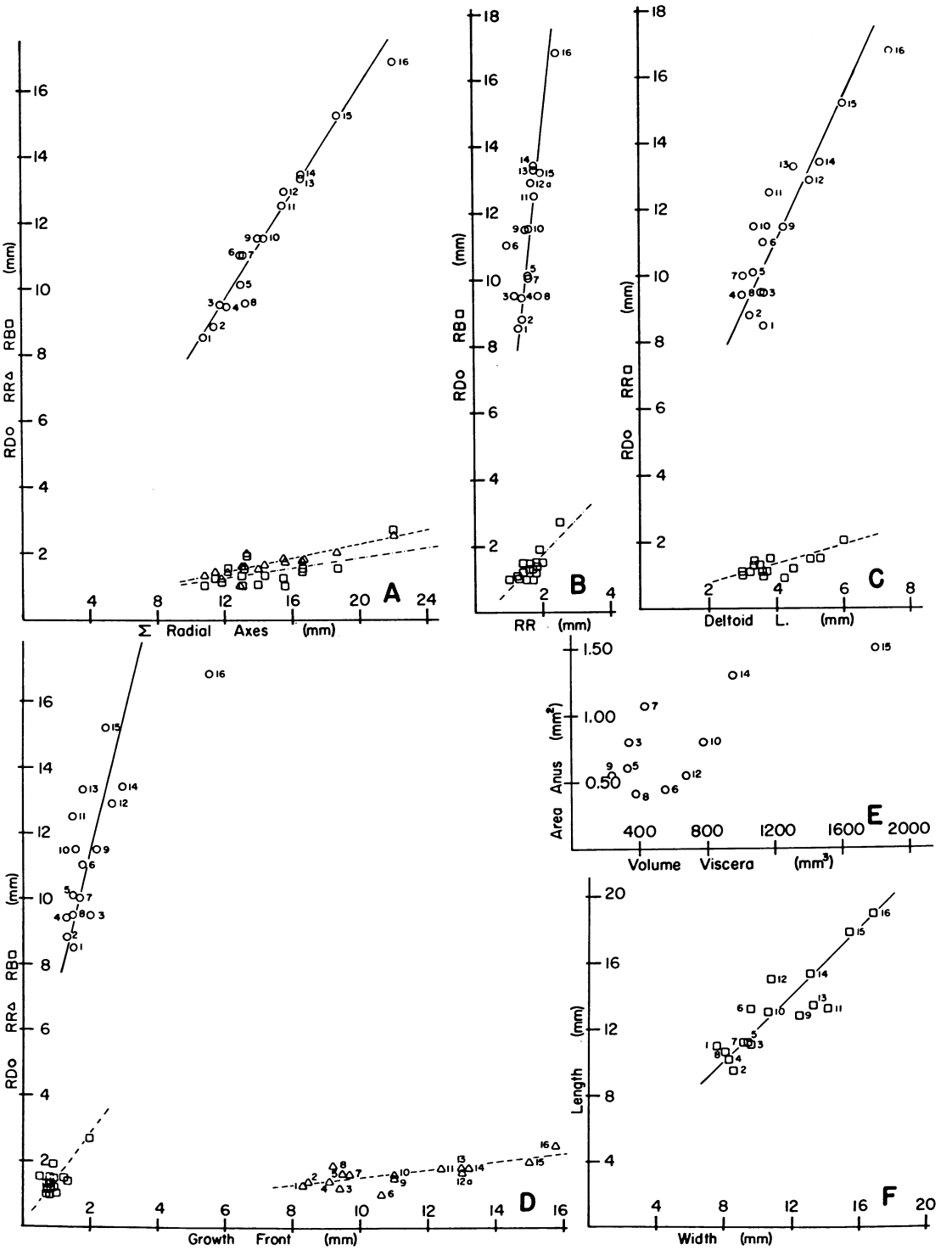
RDo RRΔ RBD (mm)
Σ Radial Axes (mm)
A
RDo RBD (mm)
RR (mm)
B
RDo RRD (mm)
Deltoid L. (mm)
C
Area Anus (mm²)
Volume Viscera (mm³)
E
RDo RRΔ RBD (mm)
Growth Front (mm)
D
Length (mm)
Width (mm)
F

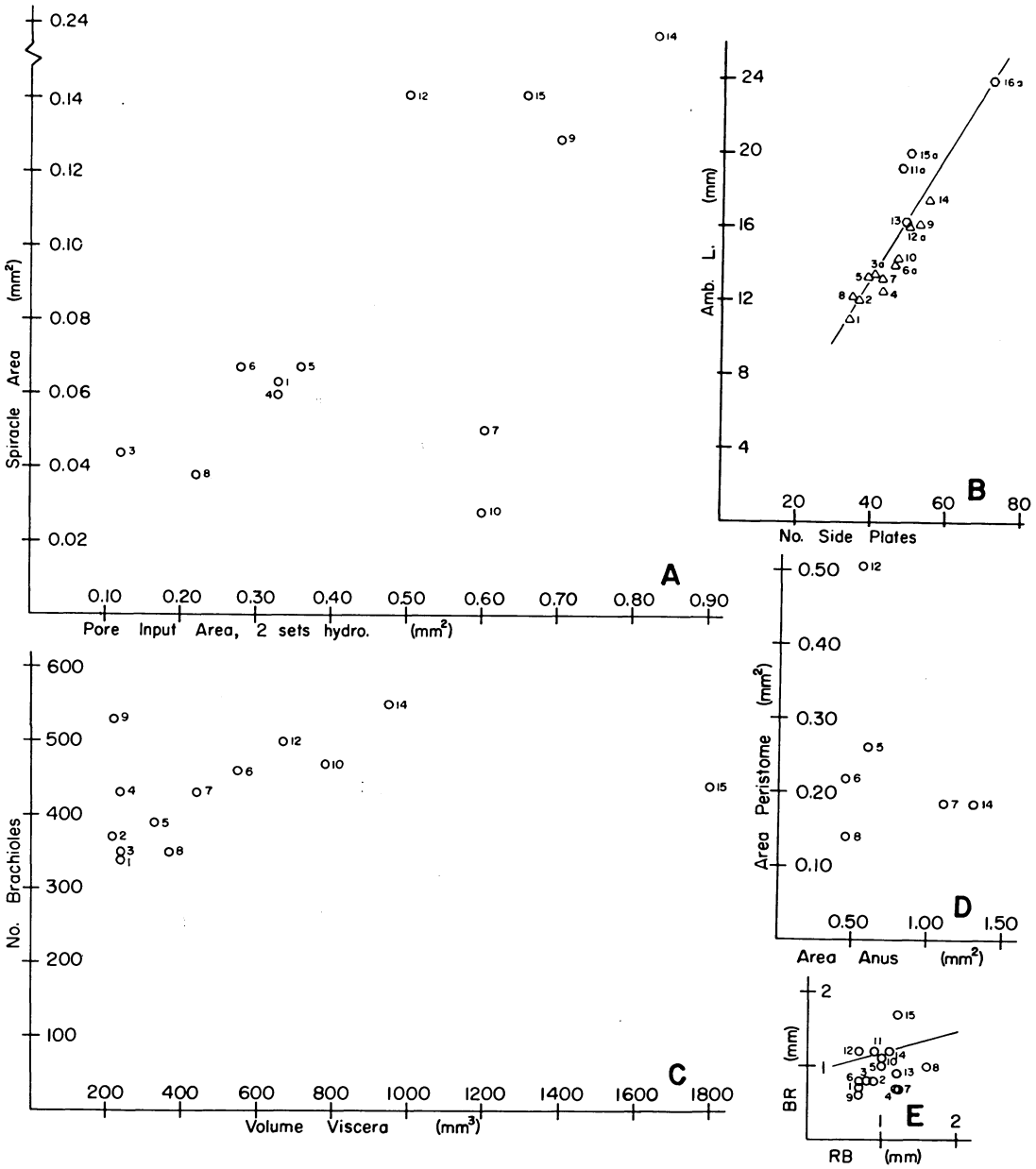

TEXT-FIG. 7 – Growth series of *Decemoblastus melonoides* (Meek and Worthen). See Text-figure 1 for explanation. *A*, Area of a single spiracle vs. pore areas along two sides of one ambulacrum; *B*, Ambulacral length vs. number of side plates along one side of ambulacrum; *C*, Total number of brachioles per specimen vs. volume of viscera; *D*, Area of peristome vs. area of anal opening; *E*, Length of BR growth axis vs. length of RB growth axis.

Remarks.– *Schizoblastus sayi* is one of the most common Burlington blastoids and some variance in shape has caused other authors to propose species which are synonyms, including *Cribroblastus verrucosus* Hambach (= *Schizoblastus sayi* var. *verrucosus* Cline – Pl. 3, fig. 14). *Pentremites potteri* Hambach (= *Schizoblastus sayi* var. *potteri* Cline – Pl. 4, figs. 15, 18), *Schizoblastus laudoni* Cline

(Pl. 4, fig. 16) and *Schizoblastus burlingtonensis* Cline (Pl. 4, fig. 17). The syntype material of *S. sayi* described by Shumard (1855) consists of a complete specimen (Pl. 3, fig. 2; Pl. 4, fig. 14), a chert mold for one side of an exterior (Pl. 4, fig. 12), and an incomplete specimen (Pl. 4, fig. 19). A complete synonymy will be found in Cline (1936) and Bassler and Moodey (1943). The point of convergence of the growth lines in the lateral sectors of the deltoid body which is aboral or just marginal to a spiracle is presumably near the junction of radial and deltoid hydrospire material. That part of the deltoid body bordering deltoid hydrospire material could not grow perpendicular to the axis of the hydrospires without causing tensional rift between it and the hydrospires or overgrowing them. It is a functional necessity that the hydrospires be formed of radial material almost to the spiracle; the deltoid is a solid plate in an interambulacral area; if this is to increase in width, it must do so laterally; since the hydrospires connect to pores along the ambulacrum, hydrospires formed from deltoids would be overgrown, rifted, and become useless (Pl. 3, fig. 7). The formation of these hydrospires from radials permits the deltoid to slip over the hydrospires as it grows laterally, leaving them intact. The number of hydrospires per group is constant at different localities in the Burlington Ls. as in Burlington, Ia. (USNM S3736), Sagetown, Ill. (USNM S3737), Curryville, Mo. (USNM S3740), and Louisiana, Mo. (USNM S3761), and the Reeds Spring Formation.

See SPECIES DIFFERENTIATION for a comparison between this and the other species assigned to *Schizoblastus*.

ACKNOWLEDGMENTS

The writer wishes to thank P. M. Kier and T. Phelan for courtesies extended while working at the Smithsonian Institution.

J. Sprinkle kindly reviewed the manuscript and offered helpful suggestions. F. Ettensohn offered helpful comments on the stratigraphy of the Broadhead and New Providence formations in Kentucky.

This research was conducted under NSF grant GB-2401.

REFERENCES

BASSLER, R. S. and M. W. MOODEY. 1943. Bibliographic and faunal index of Paleozoic pelmatozoan echinoderms. Geol. Soc. Amer. Spec. Paper 45, 733 p.

BATHER, F. A. 1899. The genera and species of Blastoidea with a list of specimens in the British Museum (Natural History). British Museum Nat. Hist., London, 70 p.

____ 1900. The Echinoderma. The Pelmatozoa *in* E. R. Lankester, A treatise on zoology. Adam and Charles Black, London, v. 3, 344 p.

____ 1908. *in* G. Boehm, Geologische Mitteilungen aus dem Indo-Australischen Archipel. Neues Jahrb. Mineral., Beil.-Band 25: 303-319.

BERGOUNIOUX, F. M. 1953. Classe des Blastoides *in* J. Piveteau, ed., Traite de Paleontologie. Masson et Cie., Paris, v. 3, p. 629-650.

BREIMER, A. and D. B. MACURDA, JR. 1972. The phylogeny of the fissiculate blastoids. Koninkl. Neder. Akad. van Weten., Verh., Afd. Nat., Eerste Reeks, Deel 26(3), 390 p.

CLINE, L. M. 1936. Osage blastoids: Part 1. The genus *Schizoblastus*. J. Paleontol., 10: 260-281.

ETHERIDGE, R., JR. and P. H. CARPENTER. 1882. On certain points in the morphology of the Blastoidea, with descriptions of some new genera and species. Ann. Mag. Nat. Hist. Ser. 5, 9: 213-252.

____ and P. H. CARPENTER. 1886. Catalogue of the Blastoidea. British Museum Nat. Hist., London, 322 p.

FAY, R. O. 1961a. *Deltoblastus*, a new Permian blastoid genus from Timor. Okla. Geol. Notes, 21: 36-40.

____ 1961b. Blastoid studies. Univ. Kansas Paleon. Contrib., Echinodermata, Art. 3, 147 p.

____ and J. WANNER. 1967. Systematic descriptions. Treatise on Invertebrate Paleontology, R. D. Moore (ed.), Part S. Echinodermata 1, p. S396-S445. Lawrence, Kansas, Univ. Kansas press and Geol. Soc. America.

HAMBACH, G. 1880. Contribution to the anatomy of the genus *Pentremites*, with description of new species. St. Louis Acad. Sci., Trans., 4: 145-160.

_____ 1903. Revision of the Blastoidea, with a proposed new classification, and descriptions of new species. St. Louis Acad. Sci., Trans., 13: 1-67.

LAUDON, L. R. 1937. Stratigraphy of northern extension of Burlington Limestone in Missouri and Iowa. Am. Assoc. Petrol. Geol. Bull., 21: 1158-1167.

MACURDA, D. B., JR. 1962. Observations on the blastoid genera *Cryptoblastus, Lophoblastus* and *Schizoblastus*. J. Paleontol., 36: 1367-1377.

_____ 1966. The ontogeny of the Mississippian blastoid *Orophocrinus*. J. Paleontol., 40: 92-124.

_____ 1967. Development and hydrodynamics of blastoids. Treatise on Invertebrate Paleontology, R. C. Moore (ed.), Part S. Echinodermata 1, p. S356-S381. Lawrence, Kansas, Univ. Kansas Press and Geol. Soc. America.

_____ 1977. *Arcuoblastus* and *Decemoblastus*, two new Mississippian blastoid genera from the Burlington Limestone, Iowa. J. Paleontol., 51: 1201-1214.

_____ 1978. The Mississippian blastoid genus *Cribroblastus*. J. Paleontol., 52: In press.

_____ and A. BREIMER. 1977. *Strongyloblastus*, a Mississippian blastoid from western Canada. J. Paleontol., 51: 693-700.

MEEK, F. B. and A. H. WORTHEN. 1861. Descriptions of new Paleozoic fossils from Illinois and Iowa. Phil. Acad. Nat. Sci., Proc. for 1861: 128-148.

_____ and A. H. WORTHEN. 1869. Remarks on the Blastoidea, with descriptions of new species. Phil. Acad. Nat. Sci., Proc. for 1869: 83-91.

MILLER, S. A. and W. F. E. R. GURLEY. 1894. Descriptions of some new species of invertebrates from the Paleozoic rocks of Illinois and adjacent states. Ill. State Mus. Nat. Hist. Bull., 3: 1-81.

OWEN, D. D. and B. F. SHUMARD. 1850. Descriptions of fifteen new species of Crinoidea from the Sub-Carboniferous limestone of Iowa, collected during the U. S. Geological Survey of Wisconsin, Iowa, and Minnesota in the years 1848-1849. Phil. Acad. Nat. Sci. Jour., n. ser., 2: 57-70.

RICE, C. L. 1972. Geologic map of the Alcorn Quadrangle, east-central Kentucky. U. S. Geol. Surv. Geol. Quad. Map 963.

ROWLEY, R. R. 1901. Two new genera and some new species of fossils from the upper Paleozoic rocks of northeastern Missouri. Amer. Geologist, 27: 343-355.

_____ 1908. The geology of Pike County (Missouri). Mo. Geol. Surv. and Water Res., 2nd ser., 8: 1-122.

_____ and S. J. HARE. 1891. Descriptions of some new species of crinoids and blastoids from the Sub-Carboniferous rocks of Pike and Marion Counties, Missouri, and Scott County, Virginia. Kansas City Scientist, 5: 113-118.

SHUMARD, B. F. 1855. Description of new species of organic remains. Mo. Geol. Surv. Ann. Rept., 1-2: 185-238.

_____ 1858. Descriptions of new species of Blastoidea from the Palaeozoic rocks of the western states, with some observations on the structure of the summit of the genus *Pentremites*. St. Louis Acad. Sci., Trans., 1: 238-248.

_____ 1866. A catalogue of the Palaeozoic fossils of North America. Part I. Palaeozoic Echinodermata. St. Louis Acad. Sci., Trans., 2: 334-407.

WANNER, J. 1924. Die Permischen Echinodermen von Timor, Teil II. Paläont. Timor, Lief 14, Abh. 23: 1-81.

WEIR, G. W. 1967. Geologic map of the Berea Quadrangle, east-central Kentucky. U. S. Geol. Surv. Geol. Quad. Map 649.

_____, K. Y. LEE, and P. E. CASSITY. 1971. Geologic map of the Bighill Quadrangle, east-central Kentucky. U. S. Geol. Surv. Geol. Quad. Map 900.

WHITE, C. A. 1877. Report upon invertebrate fossils collected in portions of Nevada, Utah, Colorado, New Mexico, and Arizona. U. S. Geog. Survey West of 100th Meridian (Wheeler), v. 4, pt. 1: 1-219.

APPENDIX 1

Localities for specimens measured in growth series.

Schizoblastus aplatus (Rowley and Hare). 14 specimens.
Rowley collection, Univ. of Illinois.
Specimens 1-11, 13. Upper Burlington Ls., Louisiana, Mo.
Specimens 12, 14. RX-36 B and E. Upper Burlington Ls., Louisiana and Curryville, Mo.

Schizoblastus marginulus (Rowley). 5 specimens. Rowley collection, Univ. of Illinois. 1: RX-209G. Burlington Ls., Louisiana, Mo.; 2: RX-209C; 3: RX-209D; 4: RX-209A; 5: RX-209B. Burlington Ls., Hart's and Pratt's quarries, Louisiana, Mo.

Schizoblastus moorei Cline. 12 specimens. Reeds Spring Fm. (type section), NW¼ SW¼ sec. 31, T24N, R22W, Stone Co., Mo.
Specimens 1-10. USNM 160642-160651.
Specimen 11. SUI 2557. Paratype.
Specimen 12. SUI 777. Holotype.

Schizoblastus sayi (Shumard)

Growth series A. 21 specimens, USNM S5464-S5484. Upper Burlington Ls., Burlington, Iowa.

Growth series B. 15 specimens. Upper Burlington Ls., lower *Physetocrinus* Zone. Quarry of Universal Atlas Portland Cement Co., NE¼ sec. 10, T56N, R4W, Ralls Co., Mo.
Specimens 1-3, 5-10, 12-15. USNM 160652-160664.
Specimens 4, 11. UMMP 62142, 62143.

Growth series C. 17 specimens, USNM 160665-160669; 248295-248306. Reeds Spring Fm. (type section), NW¼ SW¼ sec. 31, T24N, R22W, Stone Co., Mo.

Growth series D. A composite, 11 specimens from two localities in central Missouri.
D1. 6 specimens, USNM 248307-248312. Burlington Ls. Quarry, SE¼ NW¼ sec. 2, T48N, R19W, Pilot Grove North quadrangle, SE of Blackwater, Mo.
D2. 5 specimens, USNM 248313-248317. Burlington Ls., old M. K. and T. quarry, at Sweeney, 2½ miles north of Clifton City, Mo.

Growth series E. 15 specimens. Rowley collection, University of Illinois.
Upper Burlington Ls., Louisiana, Mo.

Abbreviations: SUI = State University Iowa; UMMP = University Michigan Museum Paleontology; USNM = U.S. National Museum.

EXPLANATION OF PLATE 1

Figures *1, 2, 7* – *Schizoblastus moorei* Cline. USNM 160649. Reeds Spring Fm. No. 8 in growth series (see also Pl. 2, fig. 1; Pl. 6, fig. 2). Views of hypodeltoid, oral area, and DE deltoid respectively, x 7.

Figures *3, 4* – *S. moorei.* Holotype. SUI 777. Reeds Spring Fm. No. 10 in growth series (see also Pl. 2, fig. 4). Lateral (B) and oral views respectively, x 3.

Figure *5* – *S. moorei.* USNM 160643. Reeds Spring Fm. No. 2 in growth series. Base of A ambulacrum, x 7.

Figure *6* – *S. moorei.* USNM 160646. Reeds Spring Fm. No. 5 in growth series (see also Pl. 2, fig. 3). Basal plates, azygous basal NW, x 7.

Figures *8, 10, 14* – *Schizoblastus aplatus* (Rowley and Hare). Rowley collec., Univ. Illinois. Burlington Ls. No. 6 in growth series (see also Pl. 3, figs. 6, 8; Pl. 5, fig. 9). Views of hypodeltoid, oral area, and DE deltoid respectively, x 7.

Figure *9* – *Schizoblastus sayi* (Shumard). USNM 248299. Reeds Spring Fm. No. 10 in growth series C (see also Pl. 5, figs. 2, 10, 11). View of basals, azygous basal NW, x 7.

Figure *11* – *S. aplatus.* Rowley collec., Univ. Illinois. Burlington Ls. No. 10 in growth series (see also Pl. 3, fig. 11). Inclined oral view, x 7.

Figure *12* – *S. sayi.* USNM 160663. Burlington Ls. No. 14 in growth series B. View of basals, azygous basal NW, x 7.

Figure *13* – *S. sayi.* USNM 160657. Burlington Ls. No. 7 in growth series B. View of basals, azygous basal NW, x 7.

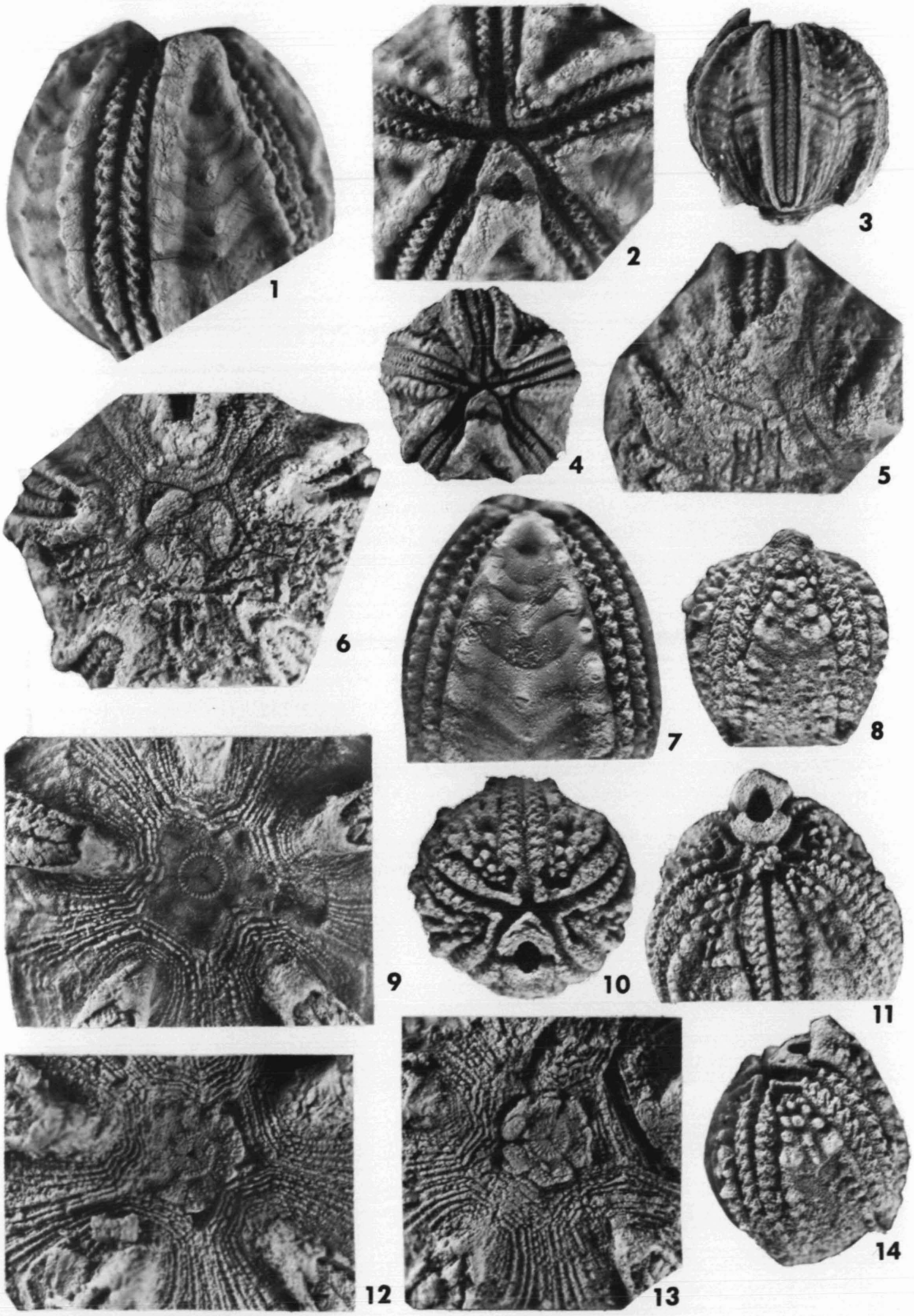
1
2
3
4
5
6
7
8
9
10
11
12
13
14

EXPLANATION OF PLATE 2

Figure *1* – *Schizoblastus moorei* Cline. USNM 160649. Reeds Spring Fm. No. 8 in growth series (see also Pl. 1, figs. 1, 2, 7; Pl. 6, fig. 2). Oral view, x 4.

Figure *2* – *S. moorei*. USNM 160647. Reeds Spring Fm. No. 6 in growth series. Lateral (D) view, x 4.

Figure *3* – *S. moorei*. USNM 160646. Reeds Spring Fm. No. 5 in growth series (see also Pl. 1, fig. 6). Basal view, x 4.

Figure *4* – *S. moorei*. Holotype. SUI 777. Reeds Spring Fm. No. 10 in growth series (see also Pl. 1, figs. 3, 4). Basal view, x 3.

Figures *5, 7* – Holotype of *Granatocrinus winslowi* Miller and Gurley 1894. Field Museum (formerly Walker Museum, 6621) = *S. moorei*? Burlington Ls.?, drift at Danville, Illinois. Oral, lateral (B), and basal views, x 3.

Figure *8* – *S. moorei*. USNM 248318. Unassigned Osagean unit, Kissling, 1960 unpublished M.S. thesis, Univ. Wisconsin. Sec. P, Unit P 11, SW¼ SW¼ sec. 2, T3S, R11W, Valmeyer, Illinois. Inclined basal view, x 3.

Figures *9, 11* – *S. moorei*. USNM S3739. Drift, Danville, Illinois. Oral, lateral (B), and basal views, x 3.

Figures *12, 14, 16 18, 21* – *Schizoblastus marginulus* (Rowley). RX-209C, Rowley collec., Univ. Illinois. Burlington Ls. No. 2 in growth series. *12, 16,* Basal and lateral (A) views, x 4. *14, 18, 21,* Oral, interambulacral, and basal views, x 7.

Figure *13* – *S. marginulus*. RX-209D, Rowley collec., Univ. Illinois. Burlington Ls. No. 3 in growth series. Oral view, x 4.

Figures *15, 17, 19 20* – *S. marginulus*. RX-209A, Rowley collec., Univ. Illinois. Burlington Ls. No. 4 in growth series (see also Pl. 6, fig. 1). *15, 17,* Oral and basal views, x 3. *19, 20,* Oral and DE deltoid views, x 7.

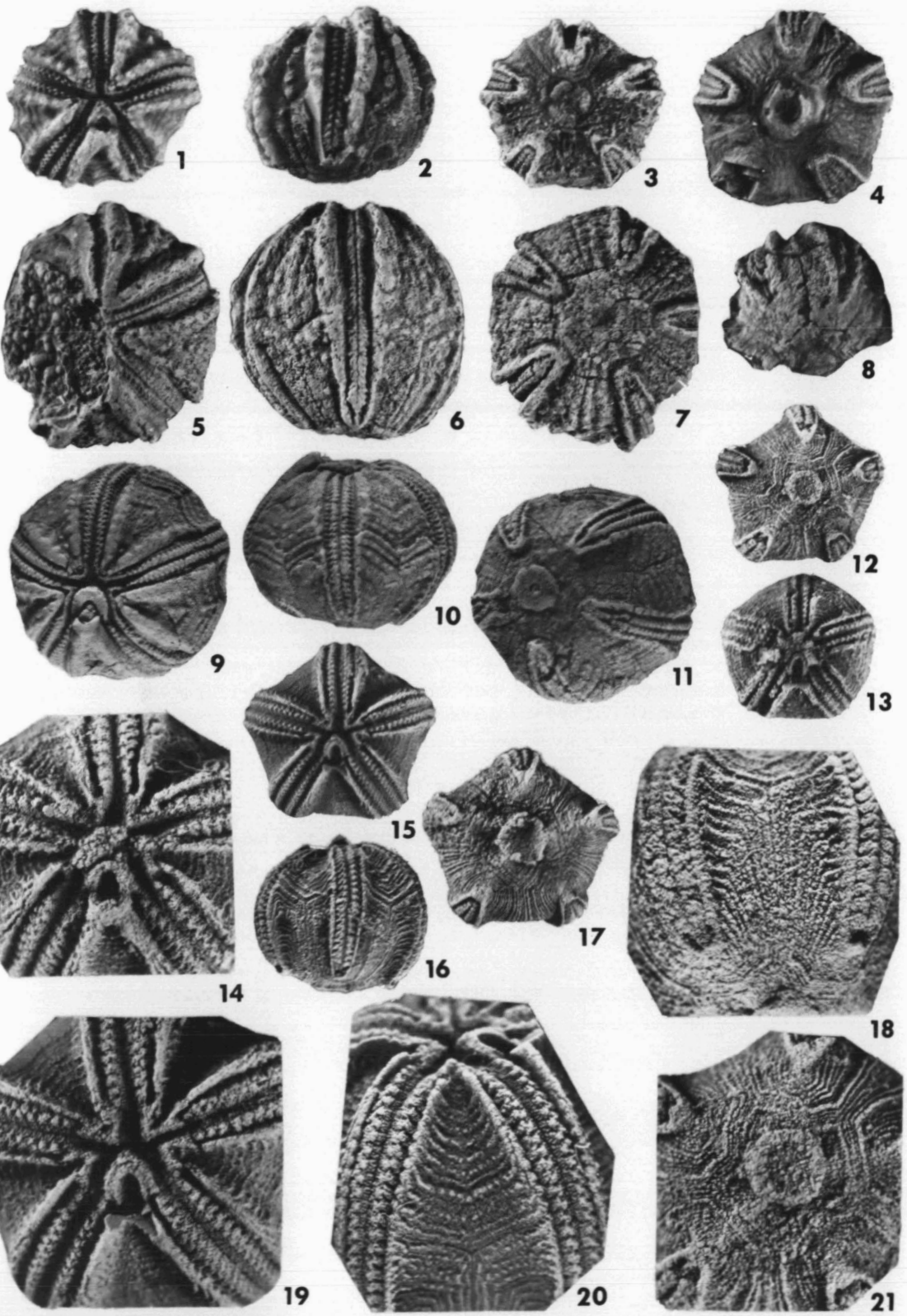
1
2
3
4
5
6
7
8
9
10
11
12
13
14
15
16
17
18
19
20
21

EXPLANATION OF PLATE 3

Figure *1* – *Schizoblastus sayi* (Shumard). Rowley collec., Univ. Illinois. Upper Burlington Ls., Bear Creek, Hannibal, Mo. (see also Pl. 5, fig. 6). Lateral view of large, diagenetically flattened specimen, x 3.

Figure *2* – *S. sayi.* Syntype. USNM S3735A. Burlington Ls., Marion Co., Mo. (see also Pl. 4, fig. 14). Oral view, x 3.

Figures *3-5* – *Schizoblastus aplatus* (Rowley and Hare). Rowley collec., Univ. Illinois. Burlington Ls. No. 9 in growth series. Oral, lateral (D), and basal views, x 4.

Figures *6, 8* – *S. aplatus.* Rowley collec., Univ. Illinois. Burlington Ls. No. 6 in growth series (see also Pl. 1, figs. 8, 10, 14; Pl. 5, fig. 9). Lateral (A) and oral views, x 4.

Figure *7* – *S. sayi.* L. M. Cline collec., SUI. Burlington Ls., Quarry of Universal Atlas Portland Cement Co., T56N, R4W, Ralls Co., Mo. Lateral view of CD interarea with hypodeltoid removed, x 3.

Figures *9-10* – *S. aplatus.* Rowley collec., Univ. Illinois. Burlington Ls. No. 4 in growth series. Basal view, x 4 and x 7, respectively.

Figure *11* – *S. aplatus.* Rowley collec., Univ. Illinois. Burlington Ls. No. 10 in growth series (see also Pl. 1, fig. 11). Inclined view of DE deltoid, x 7.

Figure *12* – *S. sayi.* USNM 248320. New Providence Fm. (mapped as Borden Fm., Weir, *et al.*, 1971; Rice, 1972) about 80 feet below top. Road on spur south of Redlick Creek and 8 miles east of Berea, Ky. Butts loc. 52a. Lateral (B) view, x 3.

Figure *13* – *S. sayi.* USNM 248321. Lake Valley Ls., Nunn Mb., 100 yards west of the quarry on the north side of Marble Canyon, N½ SW¼ SE¼ sec. 22, T16S, R10E, Alamogordo 15′ quadrangle, N.M. Lateral view, x 3.

Figure *14* – Holotype of *Cribroblastus verrucosus* Hambach = *Schizoblastus sayi* var. *verrucosus* Cline = *S. sayi.* USNM S3743. Burlington Ls., Allentown, St. Louis Co., Mo. Lateral view, x 3.

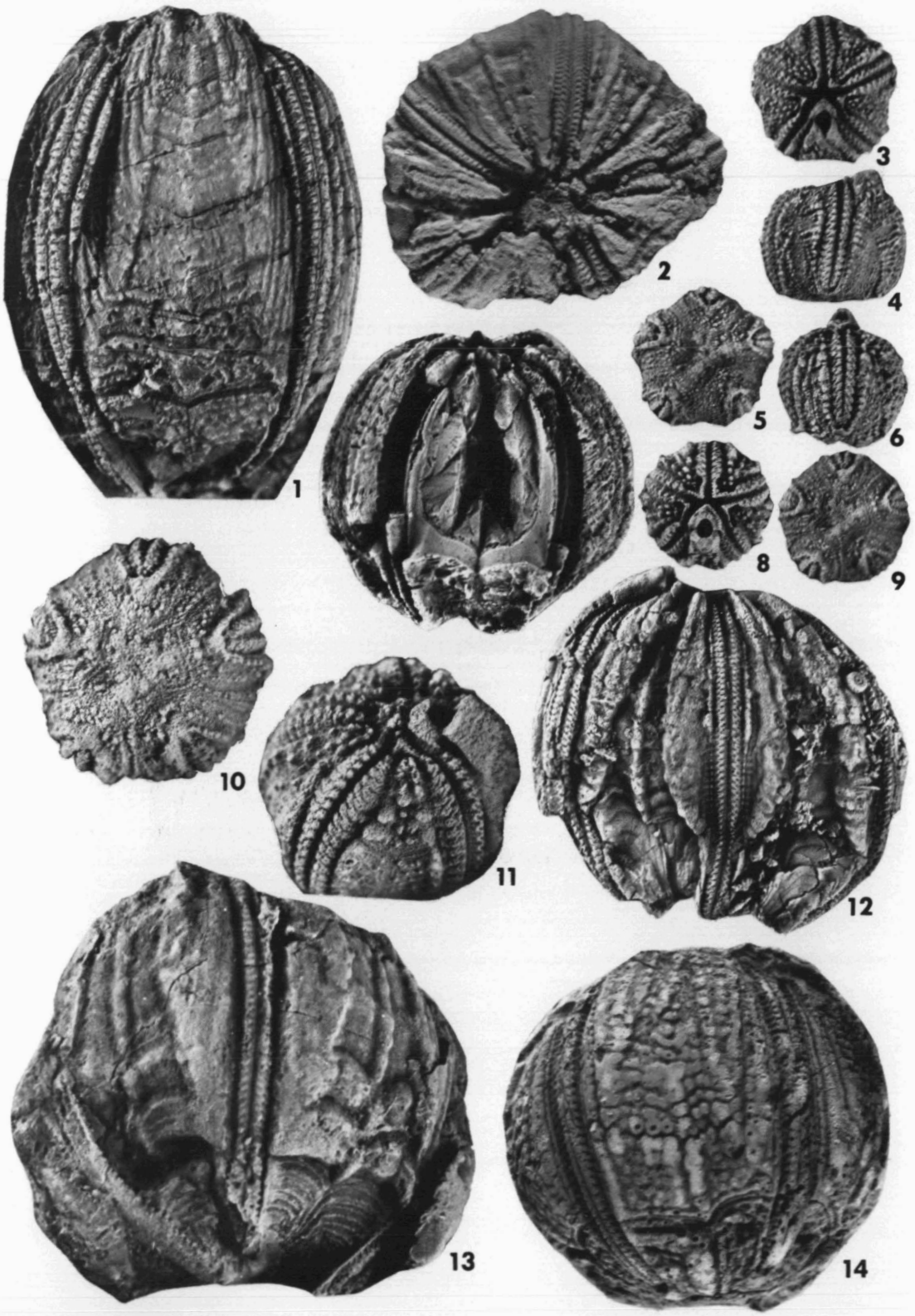
1
2
3
4
5
6
8
9
10
11
12
13
14

EXPLANATION OF PLATE 4

Figures *1-3* – *Schizoblastus sayi* (Shumard). USNM S5469. Burlington Ls. No. 6 in growth series A. Oral, lateral (A), and basal views, x 3.

Figures *4-6* – *S. sayi*. USNM S5472. Burlington Ls. No. 9 in growth series A. Oral, lateral (A), and basal views, x 3.

Figures *7, 8* – *S. sayi*. USNM S5475. Burlington Ls. No. 12 in growth series A. Oral and lateral (A) views, x 3.

Figure *9* – *S. sayi*. USNM S5476. Burlington Ls. No. 13 in growth series A. Lateral (A) view, x 3.

Figures *10, 11, 13* – *S. sayi*. USNM S5482. Burlington Ls. No. 19 in growth series A. Oral, lateral (A), and basal views, x 3.

Figure *12* – *S. sayi*. Syntype. USNM S3735B. Burlington Ls., Marion Co., Mo. View of external chert mold, x 3.

Figure *14* – *S. sayi*. Syntype. USNM S3735A. Burlington Ls., Marion Co., Mo. (see also Pl. 3, fig. 2).

Figures *15, 18* – *Pentremites potteri* Hambach = *Schizoblastus sayi* var. *potteri* Cline = *S. sayi*. Holotype. USNM S3729a. Burlington Ls., Burlington, Ia. Lateral (A) and oral views, x 3.

Figure *16* – Holotype of *Schizoblastus laudoni* Cline = *S. sayi*. SUI 778. Burlington Ls., *Physetocrinus Zone*, Dolbe Creek, SW¼ SW¼ sec. 26, T72N, R2W, Ia. Lateral (B) view, x 3.

Figure *17* – Holotype of *Schizoblastus burlingtonensis* Cline = *S. sayi*. SUI 776. Upper Burlington Ls., Burlington, Ia. Lateral (C) view, x 3.

Figure *19* – *S. sayi*. Syntype. USNM S3735C. Burlington Ls., Marion Co., Mo. Lateral view of a partial theca, x 3.

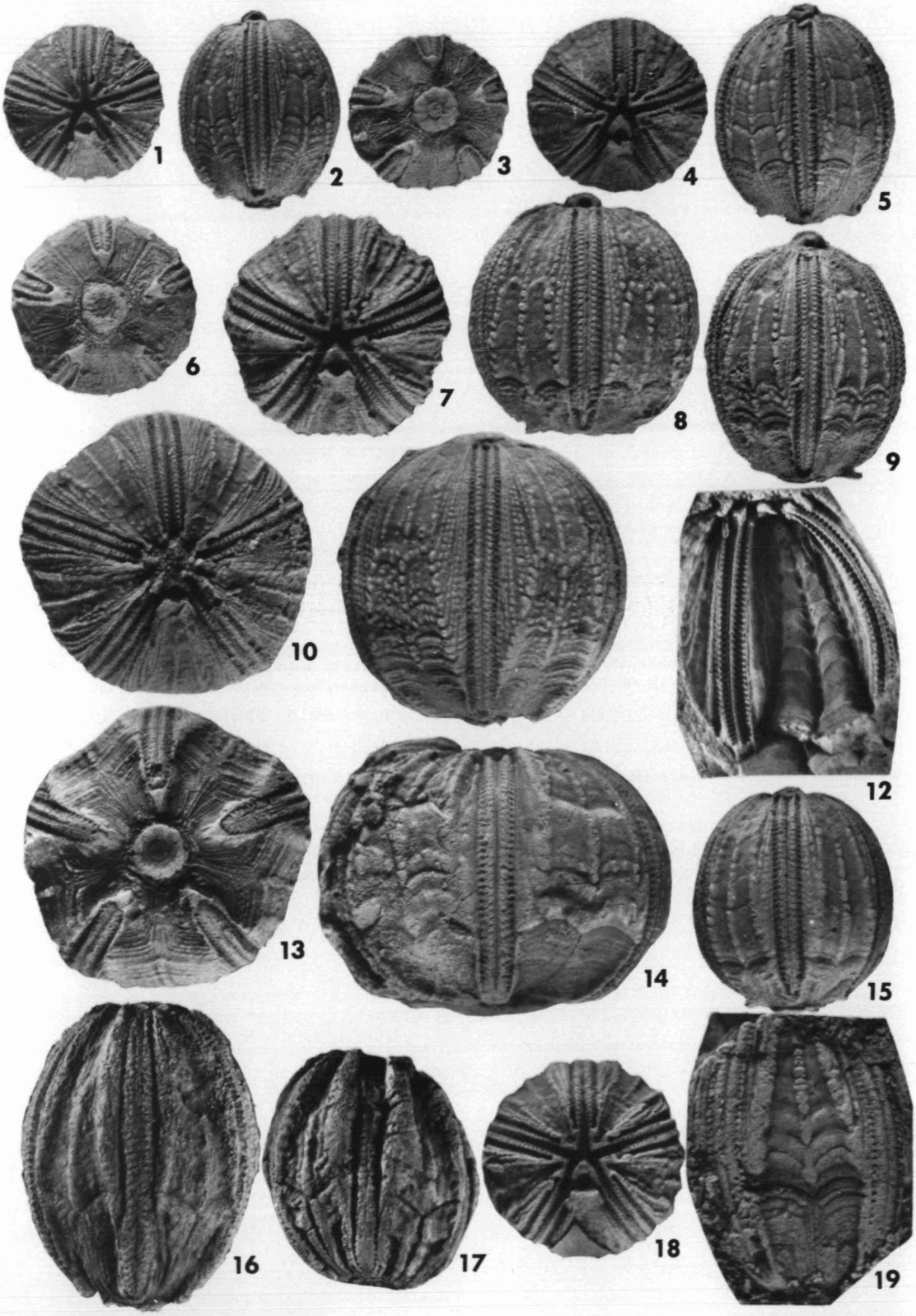
1
2
3
4
5
6
7
8
9
10
12
13
14
15
16
17
18
19

EXPLANATION OF PLATE 5

Figures *1, 4* – *Schizoblastus sayi* Shumard. USNM 248319. Burlington Ls., Hannibal, Mo. (see also Pl. 6, figs. 5, 6). Lateral view of base of hypodeltoid and aboral end of D ambulacrum, x 7.

Figures *2, 10, 11* – *S. sayi*. USNM 248299. Reeds Spring Fm. No. 10 in growth series C (see also Pl. 1, fig. 9). View of AB deltoid, origin of C radial, and oral area respectively, x 7.

Figure *3* – *S. sayi*. USNM 248302. Reeds Spring Fm. No. 13 in growth series C. View of aboral end of D ambulacrum, x 7.

Figure *5* – *S. sayi*. USNM 248298. Reeds Spring Fm. No. 9 in growth series C. Inclined view of adoral end A ambulacrum, x 7.

Figure *6* – *S. sayi*. Rowley collec., Univ. Illinois. Upper Burlington Ls., Bear Creek, Hannibal, Mo. (see also Pl. 3, fig. 1). View of medial part of ambulacrum, x 7.

Figure *7* – *S. sayi*. USNM S5339. Burlington Ls., Burlington, Ia. View of oral area of internal cast, x 7.

Figure *8* – *S. sayi*. USNM S5332. Burlington Ls., Burlington, Ia. Oral view of tetramerous mutant, x 3.

Figure *9* – *Schizoblastus aplatus* (Rowley and Hare). Rowley collec., Univ. Illinois. Burlington Ls. No. 6 in growth series (see also Pl. 1, figs. 8, 10, 14; Pl. 3, figs. 6, 8). View of D ambulacrum, x 7.

Figure *12* – *S. sayi*. Rowley collec., Univ. Illinois. Upper Burlington Ls., Louisiana, Mo. View of polygonal plates forming tube above anus from C ambulacral side, x 7.

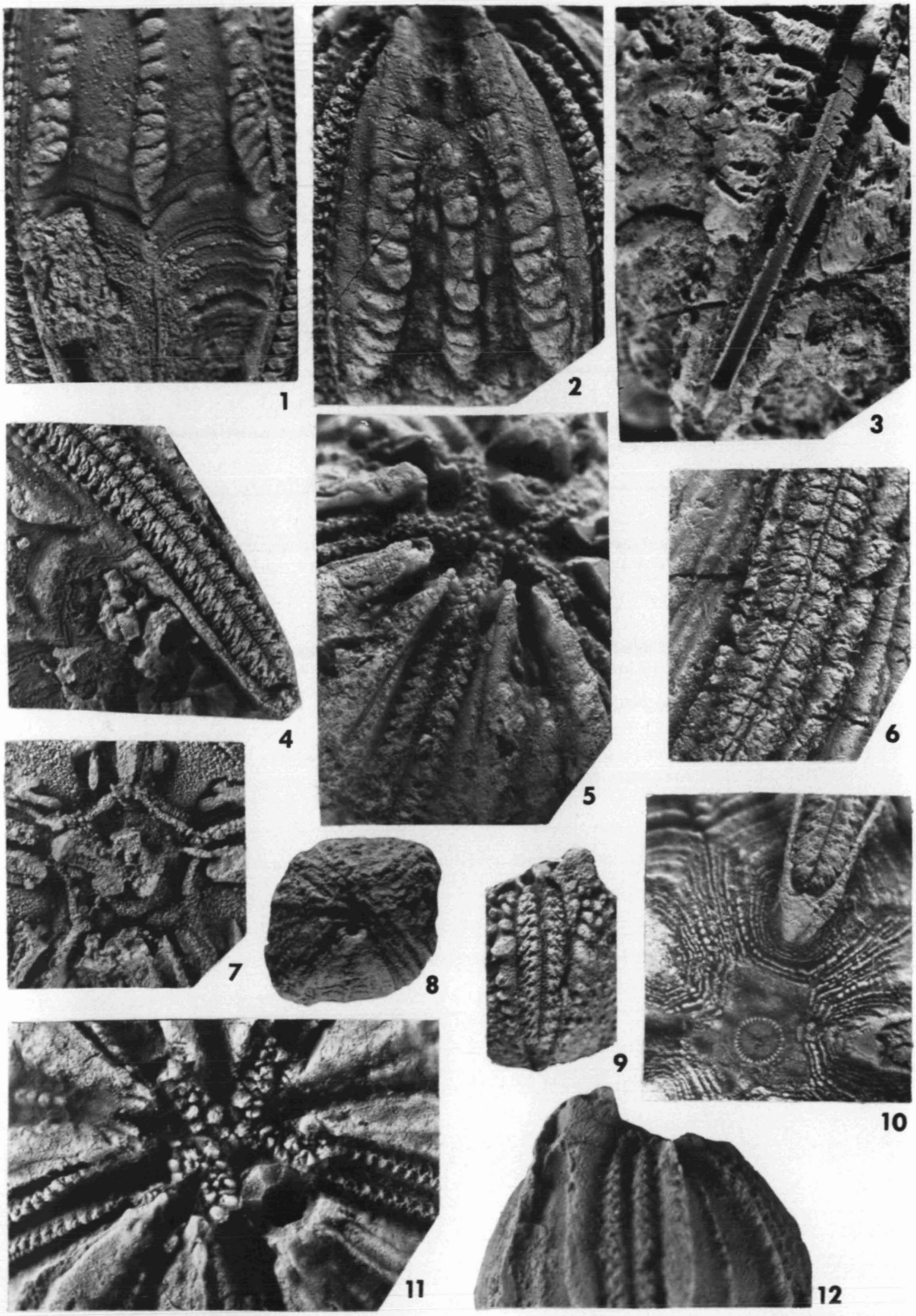
1
2
3
4
5
6
7
8
9
10
11
12

EXPLANATION OF PLATE 6

Figure *1* – *Schizoblastus marginulus* (Rowley). RX-209A, Rowley collec., Univ. Illinois. Burlington Ls. No. 4 in growth series (see also Pl. 2, figs. 15, 17, 19, 20). D ambulacrum, x 18.

Figure *2* – *Schizoblastus moorei* Cline. USNM 160649. Reeds Spring Fm. No. 8 in growth series (see also Pl. 1, figs. 1, 2, 7; Pl. 2, fig. 1). D ambulacrum, x 18.

Figure *3* – *Schizoblastus aplatus* (Rowley and Hare). Rowley collec., Univ. Illinois. Burlington Ls. No. 3 in growth series. A ambulacrum, x 18.

Figure *4* – *Schizoblastus sayi* (Shumard). USNM 160655. Burlington Ls. No. 6 in growth series B. B ambulacrum, x 18.

Figures *5, 6* – *S. sayi*. USNM 248319. Burlington Ls., Hannibal, Mo. (see also Pl. 5, figs. 1, 4). Plan and lateral views of D ambulacrum, x 18.


1

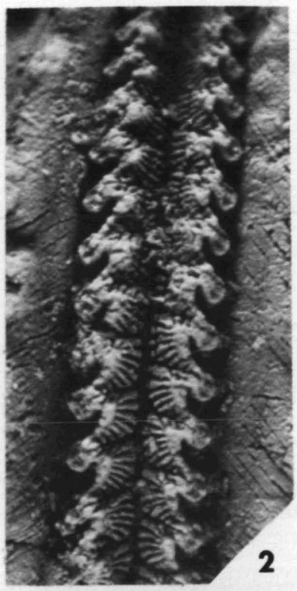
2

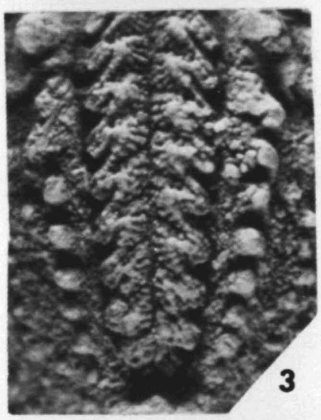
3

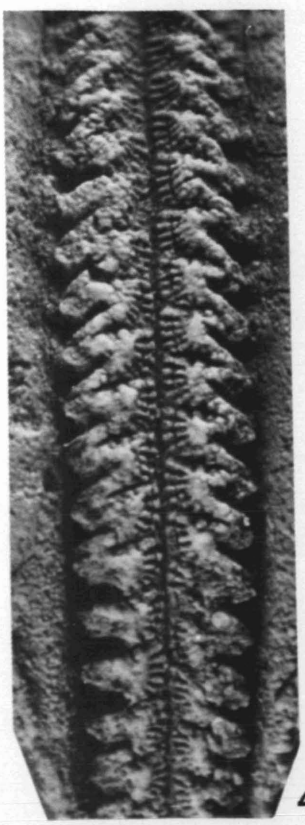
4

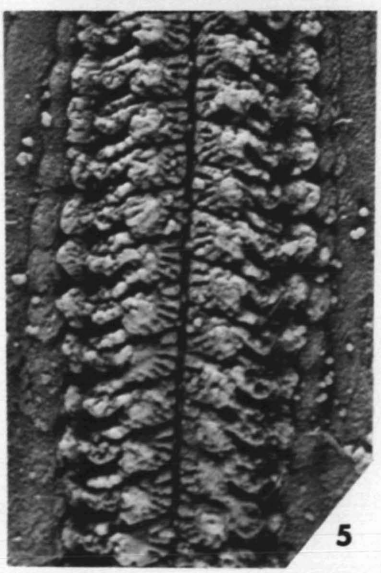
5

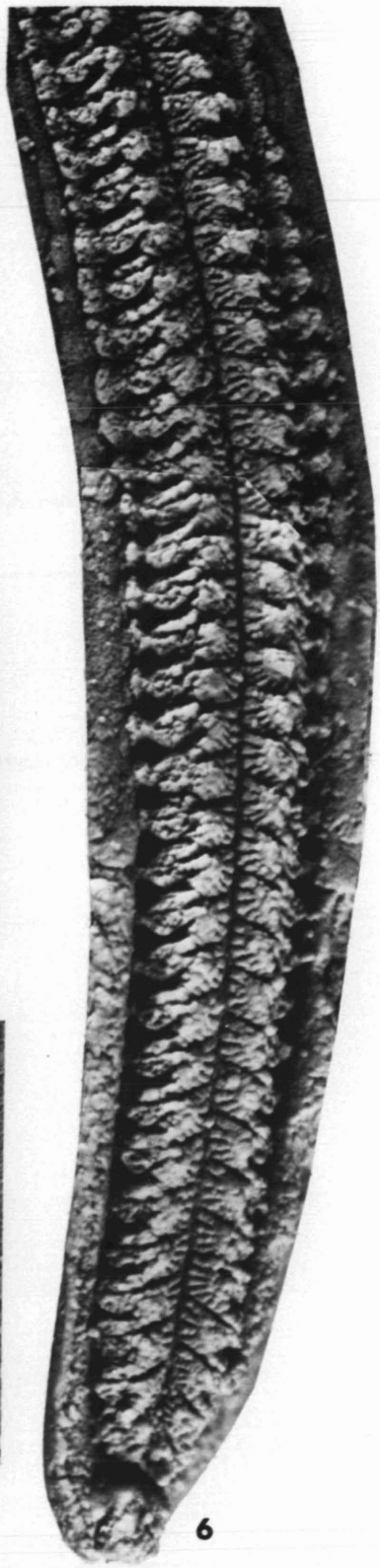
6